ANEUPLOIDY AS A CAUSE OF IMPAIRED CHROMATIN SILENCING AND MATING-TYPE SPECIFICATION IN BUDDING YEAST

by

Wahid Adam Mulla

A dissertation submitted to the Johns Hopkins University in conformity with the requirements for the degree of Doctor of Philosophy

Baltimore, Maryland

October 2017

Abstract

Aneuploidy, the state of having a chromosome number different from a multiple of the haploid number, has been associated with diseases and developmental disorders. The role of aneuploidy in human disease pathology, especially in cancer, has been a subject of much attention and debate over the last century due to the intrinsic complexity of the phenomena and experimental challenges. Aneuploidy and epigenetic alterations have long been associated with carcinogenesis, but it was unknown whether aneuploidy could disrupt the epigenetic states required for cellular differentiation.

In my PhD studies, first I did a literature review on the contribution of studies in yeast to current knowledge about aneuploidy with special emphasis on experimental features making yeast a simpler and efficient model to investigate the complex questions in the field of aneuploidy (Chapter 2). Over the last decade, yeast has been an invaluable model for driving discoveries about the genetic and molecular aspects of aneuploidy. Understanding of aneuploidy has been significantly improved owing to the methods for selectively generating aneuploid yeast strains without causing other genetic changes, techniques for detecting aneuploidy, and cutting-edge genetics and 'omics' approaches. In this review, we discuss the contribution of studies in yeast to current knowledge about aneuploidy. Special emphasis is placed on experimental features which make yeast a simpler and efficient model to investigate the complex questions in the field of aneuploidy.

In second part (Chapters 3 and 4), I performed genetic analyses revealing that purely quantitative changes in the relative copy number of chromosomes can be sufficient to disrupt the epigenetic mechanisms that define the cells' differentiated state. In this study, we found that ~3% of random aneuploid karyotypes in yeast disrupt the stable inheritance

of silenced chromatin during cell proliferation. Karyotype analysis revealed that this phenotype was significantly correlated with gains of chromosomes III and X. Chromosome X disomy alone was sufficient to disrupt chromatin silencing and yeast mating-type identity as indicated by a lack of growth response to pheromone. The silencing defect was not limited to cryptic mating type loci and was associated with broad changes in histone modifications and chromatin localization of Sir2 histone deacetylase. The chromatin-silencing defect of disome X can be partially recapitulated by an extra copy of several genes on chromosome X. These results suggest that aneuploidy can directly cause epigenetic instability and disrupt cellular differentiation.

Our findings provide the causal evidence that aneuploidy is a source of epigenetic instability. It may thus be worth exploring a potential linkage between epigenetic dysregulation and chromosome copy number alterations observed in cancer. The aneuploidy-induced changes in heterochromatin inheritance and histone-modification landscape may be an important mechanism by which chromosomal instability drives large-scale phenotypic variability during tumor evolution.

Advisor: Prof. Rong Li

Readers: Prof. Rong Li and Prof. Susan Michaelis

Dedicated to my dear parents,

Adam Mulla and Nurjahan Mulla

मेरे प्रिय माता-पिता,

आदम मुल्ला और नूरजहां मुल्ला को समर्पित

Acknowledgement

Getting Ph.D. from Johns Hopkins University will always be one of the biggest accomplishment in my entire life. I started my preliminary education in a school in a small-town India where I was only student in my class until seventh grade and the whole school was of twelve students only. Starting from there, making my way to Hopkins and finishing my Ph.D. will always be the life-changing experience. It has empowered me to dream, strive and achieve for anything. It has empowered me to hope- hope for life, hope for opportunity and hope for making the difference. All I have achieved is merely a reflection of the help and guidance that I received from many people who came into my life and will stay forever.

First, thank you Rong. I admire you so much as a scientist and as a person. You have taught how to ask meaningful questions, design simple but insightful hypothesis and test it with rigorous experiments. You have taught me organization- whether its writing paper, presenting in meetings or navigating through different experiments. Working under mentorship was a true scientific adventure, full of ups and downs. But, you were always there to make sure I was marching in the right direction. Without your support, patience, and kindness, I would not reach to a stage where I am today and recognize myself as a young scientist.

Second, thanks for my current and former lab mates both at Hopkins and Stowers Institute. You made our lab and my graduate school experience interesting and full of joy. Sree, you have been very supportive in making sure lab functions well and everyone have what they need to perform their experiments. Jin, Hung-Ji, Guangbo, Sarah, Pushpendra and Tamara, I learned a lot from you. Akshay and Linhao, I would not

have made through the coursework without you, thank you so much. Andrei, thanks for making sure that our lab goes out to eat and have fun at least once a month, and keeping our computers are safe and efficient. I am also thankful to my best friends- Hemant, Prachi, Kamalakar, Ram, Guangbo (my first PhD teacher), Tejas, Mayuri, Gunjan, Kuldeep, Maya, Atul. Speacial thanks to my dear friend Afsha for being there with me through my personal and professional adventure.

Thanks to Human Genetics program- Dr. David Valle, Dr. Kirby Smith, Dr. Haig Kazazian, Dr. Andy McCallion, and Sandy Muscelli. I really appreciate your support with the transfer for my graduate studies and all your co-operation. Special thanks to Dr. Kirby Smith, Dr. Haig Kazazian, Dr. Andy McCallion for helping me to prepare for my oral exam. I feel very proud to be a part of our Human Genetics program and training I have received here will serve throughout my life. I also want to thank classmates, you made our graduate life so much fun.

To my thesis committee- Dr. Andrew Holland, Dr. Sean Taverna, Dr. Brandon McCormick, and Dr. Susan Michaelis (committee chair), I really appreciate your and support. Special thanks to Dr. Susan Michaelis who took time to read and comment on my dissertation.

Lastly, I am very grateful to the family for their infinite and unconditional love, encouragement and support. Dad, you are my idol and inspiration. I truly admire your tireless effort to inculcate in me strong values and the noble perspective. Mom, you are always inspirational for the enormous hard work you have done for our family- whether walking miles and miles to fetch the water from the well to feeding us food you cooked using firewood for 20 years. At the end, thank god!

Table of Contents

List of Tables

List of Figures

Chapter 1

Introduction

Some contents in this chapter are adapted from:

*Mulla, W., J. Zhu and R. Li (2014). "Yeast: a simple model system to study complex phenomena of aneuploidy." FEMS Microbiol Rev **38**(2): 201-212.

Aneuploidy as a cause of impaired chromatin silencing and mating-type specification in budding yeast. Mulla WA, Seidel CW, Zhu J, Tsai HJ, Smith SE, Singh P, Bradford WD, McCroskey S, Nelliat AR, Conkright J, Peak A, Malanowski KE, Perera AG, Li R. eLife 2017.

Eukaryotic cell division is a highly complex and regulated process involving a robust surveillance mechanism, called mitotic checkpoint (or spindle assembly checkpoint), to ensure the fidelity of chromosome segregation. Alterations in the mitotic checkpoint and components of the chromosome segregation machinery often result in an unbalanced genomic state called aneuploidy (Aguilera and Gomez-Gonzalez 2008). Aneuploidy exists in somatic cells such as normal human brain (Rehen, Yung et al. 2005) and liver (Duncan 2013). Aneuploidy at the organismal level in humans generally causes embryonic lethality; however, a few viable aneuploidies cause genetic disorders such as Down's syndrome (trisomy 21) and Edwards syndrome (trisomy 18) (Nagaoka, Hassold et al. 2012). Aneuploidy has also been recognized as a common characteristic of cancer cells for more than 100 years (Boveri 1914, Holland and Cleveland 2009). Cancer is a dynamic evolutionary system where cells that can survive are continuously selected for, against a backdrop of restrictive conditions, ranging from tissue-specific growth regulators to various drug treatments. The adaptability and evolvability of cancer cells could be attributed to their genomic diversity conferred by aneuploidy and other forms of mutations (Nowell 1976, Pavelka, Rancati et al. 2010, Thomas, Fisher et al. 2013).

The implications of aneuploidy in cancer, drug resistance, pathogenicity as well as the existence of aneuploidy in normal human brain and liver are the subjects of recent attention. Considering the continual karyotypic changes and heterogeneity in aneuploid cell populations and the difficulty of separating the effect of aneuploidy from other types of genetic aberrations, the molecular mechanisms underlying diverse phenotypic effects of aneuploidy remain poorly understood. Despite the large effort devoted to the elucidation of the causes and consequences of aneuploidy, it is hindered by inherent scientific and

technical difficulties. (McGranahan, Burrell et al. 2012). The study of aneuploidy in cancer cells is complicated by the presence of numerous point mutations and a variety of other chromosomal abnormalities such as inversions and translocations. In addition, investigation of physiological and pathological effects of aneuploidy in multi-cellular organisms is limited by difficulties in generating isogenic and stable aneuploid cell populations. Adding to these difficulties are the low throughput, labor intensive and expensive methods currently available for accurate karyotyping. These experimental challenges underscore the need for model organisms and more efficient experimental techniques to facilitate the study of the diverse aspects of aneuploidy at the cellular and molecular levels.

The histone modification landscape and the associated open or closed (silenced) chromatin conformations regulate access to the genetic information by transcriptional machinery and provide a mechanism for the establishment and maintenance of stable epigenetic states in well-differentiated cells and tissues (Jaenisch and Bird 2003). Alterations in epigenetic modifications have been recognized as a key step in the initiation and progression of cancer whereby quiescent or slowly-dividing somatic cells escape their normal differentiated state and undergo precocious proliferation. (Feinberg, Ohlsson et al. 2006, Timp and Feinberg 2013, Morgan and Shilatifard 2015). However, the mechanisms underlying changes in the epigenetic-state associated with neoplastic transformation have not been fully elucidated.

Cancer progression is also associated with a wide range of genetic abnormalities, from mutations of single genes to structural or copy number alterations on the chromosomal level. Aneuploidy, an unbalanced genomic state in which the number of

chromosomes deviates from a multiple of the haploid complement, is found in over 90% of human solid tumors and 50% of hematopoietic malignancies (Mitelman, Johansson et al. 2012). Although the association of aneuploidy with cancer was noted more than a century ago, its contribution to cancer progression has only been actively explored in recent years (Boveri 1914, Holland and Cleveland 2012). Aneuploidy is correlated with complex patterns of altered gene transcription (Upender, Habermann et al. 2004, Ried, Hu et al. 2012), but its potential impact on the epigenetic state of cancer cells remains unclear due to the co-existence of the other genetic alterations in highly complex and unstable cancer genomes.

In my PhD studies, first I did a literature review on the contribution of studies in yeast to current knowledge about aneuploidy with special emphasis on experimental features making yeast a simpler and efficient model to investigate the complex questions in the field of aneuploidy. In second part, I performed genetic analyses revealing that purely quantitative changes in the relative copy number of chromosomes can be sufficient to disrupt the epigenetic mechanisms that define the cells' differentiated state.

Chapter 2

Yeast- A simple model system to study complex phenomena of aneuploidy

The contents are adapted from:

*Mulla, W., J. Zhu and R. Li (2014). "Yeast: a simple model system to study complex phenomena of aneuploidy." FEMS Microbiol Rev **38**(2): 201-212.

***correspondence author**

2.1 Abstract

Aneuploidy, the state of having a chromosome number different from a multiple of the haploid number, has been associated with diseases and developmental disorders. The role of aneuploidy in human disease pathology, especially in cancer, has been a subject of much attention and debate over the last century due to the intrinsic complexity of the phenomena and experimental challenges. Over the last decade, yeast has been an invaluable model for driving discoveries about the genetic and molecular aspects of aneuploidy. Understanding of aneuploidy has been significantly improved owing to the methods for selectively generating aneuploid yeast strains without causing other genetic changes, techniques for detecting aneuploidy, and cutting-edge genetics and 'omics' approaches. In this review, we discuss the contribution of studies in yeast to current knowledge about aneuploidy. Special emphasis is placed on experimental features which make yeast a simpler and efficient model to investigate the complex questions in the field of aneuploidy.

2.2 Introduction

Simple model organism, such as the budding yeast *S. cerevisiae* has emerged as a robust and versatile model system for studying the effects of genetic alterations (Botstein and Fink 2011). A unicellular eukaryote, the budding yeast, is particularly suitable for studying the effects of aneuploidy on cellular physiology because of its small haploid genome, divided into sixteen chromosomes, thus a well tolerance to aneuploidy. In addition, it is possible to generate isogenic aneuploid yeast strains without causing other genomic changes. Yeast studies of aneuploidy using genomics and proteomics approaches have significantly improved understanding of the causes and consequences of aneuploidy. Many yeast biochemical pathways are conserved across the higher eukaryotic species, justifying the use of yeast as a simple model system for studying complex biological processes. In this review, we summarize the contribution of studies in yeast to the current understanding of the causes and consequences of aneuploidy. A special emphasis is given to the methods for the generation of a variety of aneuploid yeast strains and karyotyping.

2.3 Causes of aneuploidy in yeast

Chromosome segregation errors are the cause of aneuploidy. Normally, the frequency of spontaneous chromosome gain or loss in laboratory strains of budding yeast is low. In standard laboratory conditions, the spontaneous loss rate of chromosome V in diploid budding yeast *S. cerevisiae* is around 2-8 per 10^6 cell divisions (Hartwell and Smith 1985, Klein 2001). Proper functioning of the mitotic spindle apparatus and the correct structural organization of the duplicated chromosomes are essential for fidelity of chromosome segregation in mitosis (Page and Snyder 1993). The spindle assembly

checkpoint serves as a surveillance mechanism to prevent chromosome missegregation in mitosis (Musacchio and Salmon 2007). Defects in any of these biological processes could compromise the accuracy of chromosome segregation producing an aneuploid progeny. Genetic screens in budding yeast have shown at least 10% of its genome is involved in the maintenance of chromosome stability (Ouspenski, Elledge et al. 1999, Smith, Hwang et al. 2004, Kanellis, Gagliardi et al. 2007, Yuen, Warren et al. 2007, Stirling, Bloom et al. 2011). These genes are referred as CIN genes since their mutations cause chromosome instability (CIN). Many of these CIN genes are known to function in processes such as kinetochore and spindle microtubule interaction, DNA replication, repair, condensation, and the spindle assembly checkpoint (Stirling, Bloom et al. 2011). It is essential to distinguish true CIN genes from genes whose mutations may not necessarily cause CIN, but pose a strong selection for certain aneuploid karyotypes that help alleviate growth deficiencies caused by gene mutations (Hughes, Roberts et al. 2000, Rancati, Pavelka et al. 2008). For example, big colonies isolated from *rnr1Δ* strain were found to have an extra copy of chromosome IX. This could be the result of a selection for the improved growth by increasing dosage of a paralogue gene *RNR3* on chromosome IX, but, the deletion of *RNR1* may not necessarily cause CIN.

Environmental stress has also been shown to induce chromosome missegregation in yeast. Exposure of the pathogenic yeast, *C. albicans,* to heat stress and antifungal drugs elevates the frequency of chromosome loss (Forche, Abbey et al. 2011). Also in *C. neoformans*, high-dose of fluconazole treatment has been suggested to cause chromosomal instability (Sionov, Lee et al. 2010). It was noticed that the high frequency (0.3 to 0.6%) at which aneuploidy occurs in *C. neoformans* under fluconazole stress could not be the

result of spontaneous aneuploidy formation. A recent study investigated how diverse stress conditions affect CIN in budding yeast through monitoring the loss of a minichromosome, many stress conditions were shown to promote CIN (Chen, Bradford et al. 2012). In particular, inhibition of the Hsp90 chaperone by various means markedly increased the loss rate of artificial chromosome compared to the stress-free culture condition. This effect was linked to a crucial role for Hsp90 in kinetochore assembly.

Another route to aneuploidy in yeast is through polyploidization. Meiosis of triploid or pentaploid cells gives rise to an almost exclusively aneuploid progeny. Mitosis of polyploid cells is also known to be error-prone. Tetraploid *S. cerevisiae* loses chromosomes at a higher rate than diploid (Mayer and Aguilera 1990). This is thought to be caused by an increased incidence of syntelic (mono-polar) kinetochore attachments, which arise due to an altered spindle geometry in tetraploids (Storchova, Breneman et al. 2006). Tetraploid *C. albicans* can undergo dramatic chromosome loss when growing on S. cerevisiae 'pre-sporulation' media and sorbose media. This often results in a diploid or near-diploid aneuploid progeny (Bennett and Johnson 2003).

2.4 The effect of aneuploidy on gene expression

Recent studies in yeast suggest that phenotypic effects of aneuploidy are directly linked to changes in the expression of many genes (Torres, Sokolsky et al. 2007, Rancati, Pavelka et al. 2008, Pavelka, Rancati et al. 2010, Chen, Bradford et al. 2012). There are several possible mechanisms by which aneuploidy could affect gene expression and phenotype (Birchler 2010, Pavelka, Rancati et al. 2010).

The effects of aneuploidy on gene expression can be divided as those proportional to DNA dosage, known as inlier changes; or those far beyond the DNA dosage, known as outlier changes. The inlier gene expression change is often moderate as it is chromosome copy-number driven and occurs to most genes encoded on aneuploid chromosomes. For example, in haploid aneuploid strains carrying an extra copy of one of the sixteen *S. cerevisiae* chromosomes (disomies), expression of most of the genes on an aneuploid chromosome was found to be increased two-fold as compared to the haploid control (Torres, Sokolsky et al. 2007). A similar observation came from analysis of a set of relatively stable aneuploid *S. cerevisiae* strains generated by triploid meiosis, where the relative level of mRNA (compared to euploid) for most of the genes encoded on aneuploid chromosomes directly correlates to the relative gene copy-number (Pavelka, Rancati et al. 2010). A direct DNA dosage effect on gene expression was observed in 23 aneuploid strains from a yeast deletion collection (Sheltzer, Torres et al. 2012). In other studies, such as in the case of fluconazole-resistant *C. albicans* isolates, the RNA expression change (compared to euploid) was found to correlate with DNA copy-number change (Bouchonville, Forche et al. 2009).

However, the impact of aneuploidy on gene expression is not limited to a simple dosage effect. Observed in every aneuploid yeast strain analyzed in our studies, there were a small number of genes with expression changes greater than the several standard deviations from the average chromosome expression change. These genes with outlier expression changes are distributed throughout the genome (Rancati, Pavelka et al. 2008, Pavelka, Rancati et al. 2010). Yeast transcriptional network analysis found that outlier genes are enriched as functional targets of the regulatory factors encoded on aneuploid

chromosomes. This implies that a substantial subset of outlier gene expression changes can be viewed as a downstream consequence of the inlier gene expression changes due to karyotype changes (Rancati, Pavelka et al. 2008).

Do apparent effects of aneuploidy on transcriptome translate to similar effects on the proteome? In *S. cerevisiae* aneuploid strains generated from triploid meiosis, quantitative proteomic analysis using multidimensional protein identification technology (MudPIT) revealed that the relative expression of most proteins encoded on aneuploid chromosomes scaled proportionally to DNA and mRNA dosage. Using the method of stable isotope labeling by amino acids in cell culture (SILAC), proteomic analysis performed in disomic budding yeast aneuploid strains arrived at a similar conclusion. However, in the latter study, approximately 20% of the proteins analyzed did not show a proportional increase in accordance with the chromosome number and the gene expression change, leading the authors to conclude that dosage compensation occurs in aneuploid yeast only for some genes. Further analysis of proteins that did not follow the trend of copy-number change showed that a majority of these proteins were components of various protein complexes (Torres, Dephoure et al. 2010). Although the mechanism underlying the observed dosage compensation remains to be elucidated, it may have something to do with reduced stability of proteins when they are not incorporated in their native complex.

2.5 Phenotypic effects of aneuploidy

The euploid chromosome number in a given species is an optimum acquired during evolution of that species. Generally, aneuploidy is not well tolerated in nature, manifested by impaired fitness at the cellular and organismal level. Systematic analysis of budding

yeast disomic strains showed slower cell proliferation under normal conditions compared to euploid strains (Torres, Sokolsky et al. 2007). Similar poor proliferative capacity under standard growth parameters is exhibited by aneuploid strains generated from triploid meiosis in *S. cerevisiae* and *S. pombe* (Niwa, Tange et al. 2006, Pavelka, Rancati et al. 2010). Studies in *S. cerevisiae* and *S. pombe* aneuploid strains have shown that aneuploidy causes delay in the G1 phase of their cell cycle. (Niwa, Tange et al. 2006, Torres, Sokolsky et al. 2007, Pavelka, Rancati et al. 2010). Recent study has characterized the G1 delay in aneuploid cells as a consequence of slower accumulation of G1 cyclins (Thorburn, Gonzalez et al. 2013).

Even though aneuploidy impairs growth and fitness under stress-free conditions, its adaptive value becomes apparent under conditions detrimental to euploid yeast strains. Emerging evidence suggests that aneuploidy is a form of genome alteration that promotes adaptive evolution of cells in response to harsh environments or genetic perturbations (Table 1). For example, certain aneuploid karyotypes in budding yeast enable them to overcome nutrient limitations such as low glucose, high-phosphate, or sulphate media (Gresham, Desai et al. 2008). In pathogenic fungi, aneuploidy is known to be widely associated with drug resistance and increased pathogenicity (Polakova, Blume et al. 2009, Sionov, Chang et al. 2009, Hu, Wang et al. 2011, Silva, Negri et al. 2012) (Morrow and Fraser 2013).

The adaptive benefits of aneuploidy can be attributed to the altered dosage of single or multiple genes on an aneuploid chromosome. For example, in the systematic analysis of 38 aneuploid *S. cerevisiae* strains, some aneuploid variants showed improved fitness compared to parental euploid strains under adverse conditions such as treatment with the

tumorigenic compound 4-nitroquinoline-oxide (4-NQO). The improved fitness in the presence of 4-NQO was attributed to the increased expression of the gene *ATR1*, whose copy-number was increased through the gain of chromosome XIII (Pavelka, Rancati et al. 2010). *ATR1* encodes a transporter protein known to confer 4-NQO-resistance when overexpressed (Mack, Gompel-Klein et al. 1988). Another example is radicicol resistance associated with chromosome XV gain in *S. cerevisiae*. This was attributed to the synergistic effect of the increased dosage of two genes, *STI1* and *PDR5* (encoding an Hsp90 co-chaperone and a drug pump, respectively), encoded on chromosome XV (Chen, Bradford et al. 2012).

A very remarkable adaptive effect of aneuploidy in budding yeast was observed in the case of *myo1*Δ. *MYO1* encodes the myosin-II motor protein that normally drives bud neck constriction during cytokinesis. Whereas deletion of *MYO1* results in massive cytokinesis failure and lethality in most cells (Tolliday, Pitcher et al. 2003), a few *myo1*Δ survivors were able to evolve alternative cytokinesis mechanisms through changes in chromosome stoichiometry. One class of the *myo1*Δ "evolvants" restores cytokinesis by cell wall thickening in the bud neck region, upregulating the set of genes involved in the cell wall biogenesis. Located on both euploid and aneuploid chromosomes, many of these showed outlier gene expression (Rancati, Pavelka et al. 2008). Further analysis demonstrated that these gene expression changes were due to extra copies of two genes - *RLM1* (a transcription factor) and *MKK2* (activator of *RLM1*) located on chromosome XVI. By simply introducing extra copies of *RLM1* and *MKK2* into *myo1Δ* the evolved mechanism of cytokinesis was recapitulated. Well-annotated functional genomics data in yeast have been particularly helpful in unraveling the molecular mechanisms by which an

aneuploid karyotype confers a particular phenotype. In aneuploid cancer cells, identifying specific genes on an aneuploid chromosome that could account for the growth advantage is more challenging.

2.6 Aneuploidy and chromosomal instability in yeast

While aneuploidy is a product of chromosome instability, it also correlates with elevated chromosomal instability observed as gaining or losing chromosomes at a high frequency. This vicious cycle is thought to underlie cancer "genome chaos" (Potapova, Zhu et al. 2013). Studying the relationship between aneuploidy and chromosomal instability in cancer cells is complicated by the presence of a variety of other genetic changes. Therefore, a simple and genetically tractable model system, such as yeast, holds many advantages for studying this phenomenon. The observation of chromosomal instability in aneuploid yeast cells was made more than four decades ago (Parry and Cox 1970). Extra chromosomes in aneuploid strains generated from triploid meiosis were found to have higher loss rate, generating karyotypically diverse cell populations (St Charles, Hamilton et al. 2010). High rates of chromosomal instability were also seen in aneuploid *C. albicans* strains exposed to stresses of routine experimental techniques such as transformation (Bouchonville, Forche et al. 2009). Recently, the link between chromosomal instability and aneuploidy was addressed systematically using several approaches. The rate of chromosome missegregation inferred from the loss of artificial chromosome was found to increase in 9 out of 13 yeast disomic strains (Sheltzer, Blank et al. 2011). Similarly, monosomic budding yeast cells showed an increased chromosomal instability and were predisposed to return to a diploid karyotype when cultured under

standard conditions (Waghmare and Bruschi 2005, Chen, Bradford et al. 2012). For example, chromosome XVI monosomic strain was found to be karyotypically unstable under normal conditions but when maintained under tunicamycin selection, it appeared stable in terms of population homogeneity. This underscores the challenge of finding the right conditions to separate selection vs. intrinsic genomic stability (Chen, Bradford et al. 2012). A recent study demonstrated a positive correlation of chromosome instability with the degree of aneuploidy as well as with the presence of specific aneuploid chromosomes and dosage imbalance between specific chromosome pairs (Zhu, Pavelka et al. 2012). The "genome chaos" created by aneuploidy-associated chromosome instability may be a powerful mechanism for the rapid generation of karyotypic diversity in the population, providing the substrate for evolutionary selection of adaptive genomes (Nowell 1976, Merlo, Pepper et al. 2006, Selmecki, Forche et al. 2006, Rancati, Pavelka et al. 2008, Selmecki, Dulmage et al. 2009, Chen, Bradford et al. 2012).

2.7 Experimental approaches in the study of aneuploidy using yeasts as a model organism.

2.7.1 Methods for generating aneuploidy in yeast

Several different methods have been developed to generate aneuploidy in yeast. One method for obtaining aneuploid budding yeast strains with random chromosome stoichiometry is treatment with the low concentration of radicicol, which disrupts the normal kinetochore function (Chen, Bradford et al. 2012). When a diploid strain was treated with 20 μg/ml radicicol for two days, about one third of the population was found to be an aneuploid with diverse karyotypes (Chen, Bradford et al. 2012). This is one simple

way to generate yeast aneuploid strains as it does not require a complicated genetic manipulation. Another efficient way for obtaining random aneuploid strains is by sporulation of polyploid strains with an odd ploidy. This method takes advantage of the fact that in triploid and pentaploid strains, homologous chromosomes segregate randomly in the first meiotic division thereby giving rise to mostly aneuploid spores (Fig. 1a). It has been used successfully in generating budding yeast strains with diverse karyotypes and for generating fission yeast with disomy III (Niwa and Yanagida 1985, Niwa, Tange et al. 2006, Rancati, Pavelka et al. 2008, Charles, Hamilton et al. 2010, Pavelka, Rancati et al. 2010). As discussed above, aneuploid strains derived from this method have various levels of karyotypic instability; relatively stable karyotypes could be obtained by screening for strains with low level of intra-population karyotype heterogeneity (Pavelka, Rancati et al. 2010, Zhu, Pavelka et al. 2012).

Defined aneuploid strains with simple karyotypes could be obtained by two other means. One is through the use of a conditional centromere where a *GAL1* promoter is inserted adjacent to centromere sequences (Hill and Bloom 1987, Reid, Sunjevaric et al. 2008, Anders, Kudrna et al. 2009). The transcriptional induction of the promoter abrogates centromere function and causes chromosome nondisjunction (Fig. 1b). Both disomies and monosomies have been isolated using this approach. Another method for isolating disomies is through chromoduction (Conde and Fink 1976, Nilsson-Tillgren, Petersen et al. 1980, Torres, Sokolsky et al. 2007). This method utilizes the rare chromosome transfer between two haploid strains during abortive mating (Fig. 1c). The disomic chromosome can be selected by introducing selectable markers to both homologs, although this selection prevents only the loss but not the gain of disomic or any other yeast chromosomes in the

strain. Strains with complex and simple aneuploid karyotypes have proven to be complementary in the study of the aneuploidy. Of practical note, because of the intrinsic instability of aneuploid strains, it is essential to frequently check the karyotype (see methods below) of the strains during passages and especially after revival from frozen stocks.

2.7.2 Methods for detection of aneuploidy in yeast

Recently developed genomic analysis techniques have advanced our ability to monitor karyotype changes and determine chromosome copy-numbers in yeast. Here we discuss various approaches used to detect whole chromosomal aneuploidy. These approaches include electrophoresis-based methods, flow cytometry, array-comparative genomic hybridization (a-CGH), qPCR karyotyping and Next-Generation sequencing. Besides the determination of chromosome copy-number variations, these karyotyping methods allow assessment of the size of chromosomes, genome size and ploidy level, study of genome dynamics, identification of gross chromosomal rearrangements and associated chromosomal polymorphism. Considering the scope of this article, these methods are focused for karyotyping yeast cells but are generally applicable to other eukaryotic organisms as well.

Electrophoresis based karyotyping: Pulsed-field gel electrophoresis (PFGE) has been widely used in epidemiological studies of pathogenic yeasts and optimized for the separation of *C. albicans* and *S. cerevisiae* chromosomes (Doi, Homma et al. 1992, Maringele and Lydall 2006). Although PFGE has been mainly used to detect gross chromosomal rearrangements (Pardo and Aguilera 2012, Reis, Batista et al. 2012), quantitative southern blotting after the separation of chromosomes by PFGE can be used

to detect alterations in the relative copy-number of different chromosomes (Chen, Magee et al. 2004, Bouchonville, Forche et al. 2009). Detailed protocol can be obtained from the cited reference (O'Brien, Udo et al. 2006). Another method for chromosome copy-number determination is the multiplex PCR method with micro-capillary electrophoresis where chromosomal DNA is separated based upon size to charge ratio in the interior of a small electrolyte filled capillary. Further, using a bioanalyzer, aneuploidy in the test sample can be determined by the relative ratio of the peak height of the test and euploid control DNA fragments in the chromatogram (Arbour, Epp et al. 2009).

Flow cytometry: Flow cytometry is a convenient and least expensive method for assessment of ploidy variation in the population. This technique provides an overview of cellular DNA content rather than information on the gain or loss of specific chromosomes. Estimation of DNA content is based on the use of an intercalating fluorescent dye such as SYTOX® Green dye, that binds proportionally to DNA, allowing estimation of DNA cell cycle distribution and ploidy for thousands of cells per second. This method has been optimized and routinely used for both *Candida* and *Saccharomyces* species. Detailed protocol can be obtained from cited reference (Haase and Lew 1997, Ibrahim, Magee et al. 2005, Darzynkiewicz, Halicka et al. 2010, Zhu, Pavelka et al. 2012). This technique is also highly adaptable to a high-throughput format.

Array-comparative genomic hybridization (a-CGH): Whereas, electrophoresis and flow cytometry-based methods allow for a rapid detection of aneuploid genome, a-CGH provides a high-resolution map of both DNA copy-number changes and possible structural chromosomal aberrations (Pinkel and Albertson 2005). In typical a-CGH measurements, total genomic DNA from a test sample and a normal reference sample are hybridized to an

array of fluorescent probes the spanning the entire genome. The fluorescence intensity is then measured and compared to reference samples, indicating chromosome copy-number changes as well as the gain or loss of specific loci. A variety of studies have used this method to monitor whole and segmental chromosomal aneuploidy (Pinkel and Albertson 2005, Torres, Sokolsky et al. 2007, Rancati, Pavelka et al. 2008, Arbour, Epp et al. 2009, Selmecki, Dulmage et al. 2009, Pavelka, Rancati et al. 2010, Chen, Bradford et al. 2012). Detailed protocol can be referred from cited reference (Dion and Brown 2009).

qPCR-karyotyping: Although a-CGH offers a high resolution map of the genome; its limitations include low-throughput, high costs and cumbersome sample preparation. qPCR-based karyotyping is a more convenient and high-throughput, although less accurate method for monitoring whole chromosome aneuploidy. The existing protocol employs primers recognizing a non-coding region of each arm of a chromosome and the amplified PCR product can be detected using several fluorescent intercalating dyes, such as SYBR® Green in a real-time manner. With the use of liquid handling robotics, the entire procedure, from genomic DNA extraction to the q-PCR, can be easily performed in a high-throughput format. This method has been used successfully in several yeast aneuploidy studies (Pavelka, Rancati et al. 2010, Chen, Bradford et al. 2012, Zhu, Pavelka et al. 2012).

Next Generation sequencing (NGS)-karyotyping: NGS-karyotyping is based upon massive parallel sequencing of the whole yeast genome. In brief, genomic DNA is used to create a library of smaller fragments, and then sequenced by millions of parallel reactions generating nucleotide reads. The differential coverage abundance across segments of the reference genome is used to detect chromosome copy-number variation (Dudarewicz, Holzgreve et al. 2005, Didelot, Bowden et al. 2012, Nekrutenko and Taylor 2012). Beside

copy-number information, determination of single-nucleotide polymorphisms (SNP) by sequencing also allows consideration of whether the presence SNP contributes to phenotypic changes associated with an aneuploid strain. (Rancati, Pavelka et al. 2008, Pavelka, Rancati et al. 2010, Torres, Dephoure et al. 2010). The throughput of Next Generation sequencing machines has improved dramatically over the past few years. A recent study revealed the genotyping of 1000 yeast strains, at the cost of less than 15 euros per sample, in a few weeks (Wilkening, Tekkedil et al. 2013). Also due to the recent development of single-cell whole genome amplification of an individual human cell, high coverage single-cell sequencing is now possible (Zong, Lu et al. 2012).

2.8 Future Perspective

In this review, we discussed recent progress in understanding of the causes and consequences of aneuploidy through studies in yeast. We also highlighted the methods to generate and detect aneuploidy in yeast. Yeast has proven to be a useful model in studying aneuploidy on account of it's the powerful genetics. For instance, the gain of chromosome XVI converts a budding yeast colony from 'fluffy' to 'smooth' morphology. Further, the gene responsible for the phenotypic switch was easily identified (Tan, Hays et al. 2013). This exemplifies the benefit of a well annotated functional genomics data and plasmid library of yeast genome (Hvorecny and Prelich 2010) in unraveling the molecular mechanism by which an aneuploid karyotype confers a particular phenotype.

However, many questions remain unanswered. For example, as a large portion of yeast CIN genes involved in cellular pathways are not connected to chromosome stability, additional mechanisms have yet to be identified that would lead to aneuploidy (Stirling,

Bloom et al. 2011). Existing data has clearly demonstrated the adaptive potential of aneuploidy under acute stress, but whether aneuploidy could contribute to long term adaptive evolution is less clear. A recent experimental evolution study suggested that aneuploidy *per se* might not serve as a stable and sustainable evolutionary solution (Yona, Manor et al. 2012). Yona *et al.* observed that when diploid budding yeast growing under heat and high pH conditions, aneuploids were observed first but were eventually replaced by gene mutations. Thus, aneuploidy may be a quick and rough fix under strong selective pressure, allowing sufficient propagation of the population for the emergence of adaptive mutations with less fitness cost than aneuploidy. Giving the constantly changing environment where unicellular organisms live, it is tempting to speculate that natural selection might favor the evolution of mechanisms that would modulate chromosome segregation fidelity based on the presence of environmental stress, such as critically involving a stress-handling chaperone (Hsp90) in kinetochore function.

Another key question is to what extent the knowledge we have gained about aneuploidy in yeast can be applied to multicellular organisms? As chromosome segregation is a highly conserved cellular process in eukaryotes, it is safe to say that the mechanisms of CIN in yeast could also be applied to human. Multicellular organisms may respond differently to aneuploidy as compared to yeast. For instance, whole chromosome aneuploidy is largely detrimental in multicellular species (Williams, Prabhu et al. 2008). At the cellular level, it has been suggested that the proliferation of aneuploid mouse and human cells could be limited through the *p53* pathway which do not exist in yeast (Belyi, Ak et al. 2010, Thompson and Compton 2010). Nonetheless, most cancer cells inactivate the *p53* pathway and could evolve through the production of aneuploidy (Belyi, Ak et al.

2010, Navin, Kendall et al. 2011). Besides aneuploidy, cancer cells also hold mutations and epigenetic deregulation. Yeast will remain a useful experimental model for future elucidation of the interplay between small and large genetic changes and their influence on the epigenome and vice versa, explored in chapter 3.

2.9 Figure legends:

2.9.1 Figure 1: Experimental methods for the generation of aneuploidy in yeast.

(a) Generation of aneuploidy via triploid meiosis: A triploid (*3N*) yeast cell undergoes meiosis I with random segregation of homologous chromosomes. At the end of the first meiotic division, two aneuploid progenies are formed. Second meiotic divisions produce four highly aneuploid progenies.

(b) Generation of aneuploidy via conditional centromere: The endogenous centromere of the target chromosome is replaced with a conditional centromere construct P_{GAL1}-*CEN3* in a haploid yeast cell. Galactose induces *GAL1* promoter activity causing temporary inactivation of the centromere; further results in nondisjunction of the target chromosome. Following cell division, an aneuploid cell (*N+1*) containing an extra copy of the target chromosome can be obtained.

(c) Generation of aneuploidy using a karyogamy-defective strain: A haploid (*N*) yeast strain (*kar1Δ15*) is crossed with a wild type haploid yeast strain. Occasionally, a chromosome is transferred from one nucleus to the other during abortive mating. An aneuploid (*N+1*) cell can be selected using selection markers present on each of the homologous chromosomes. (Abbreviations: *N*, chromosome number).

2.9.2 Figure 2: Characteristic examples of karyotyping methods.

(a) Karyotypic analysis of five D9-3.3 single colonies of C. albicans followed by southern hybridization to a CEN5 probe: The isochromosome 5 i(5L) hybridized to a CEN5 probe is detected in a clone D. Figure is adopted from (Selmecki *et al.*, 2009).

(b) Ploidy analysis of a budding yeast aneuploid strain RLY 4938 by FACS: A characteristic shift in G1 peak observed in an aneuploid strain RLY 4938 compared to the haploid control indicating an increased DNA content.

(c) Karyotypic analysis of an aneuploid strain RLY 4938 by a-CGH: Extra copy of chromosomes I, II, VIII, XI and XIII is detected. Hybridization intensities from all 16 chromosomes and the mitochondrial genome are plotted as $\log_2$ ratios compared to the haploid strain. Upper and lower boundaries are truncated at a $\log_2$ ratio of +1 and −1, respectively. The location of repetitive elements is indicated at the bottom with vertical bars. Figure is adopted from (Pavelka *et al.*, 2010).

(d) Karyotypic analysis of an aneuploid strain RLY 4938 by qPCR: An absolute copy number of sixteen yeast chromosomes is plotted. Extra copy of chromosomes I, II, VIII, XI and XIII is observed.

(e) Karyotypic analysis an aneuploid strain RLY 4938 by Next-Generation sequencing: A normalized median read showing extra copy of chromosomes I, II, VIII, XI and XIII.

2.9.1 Figure 1: Experimental methods for the generation of aneuploidy in yeast.

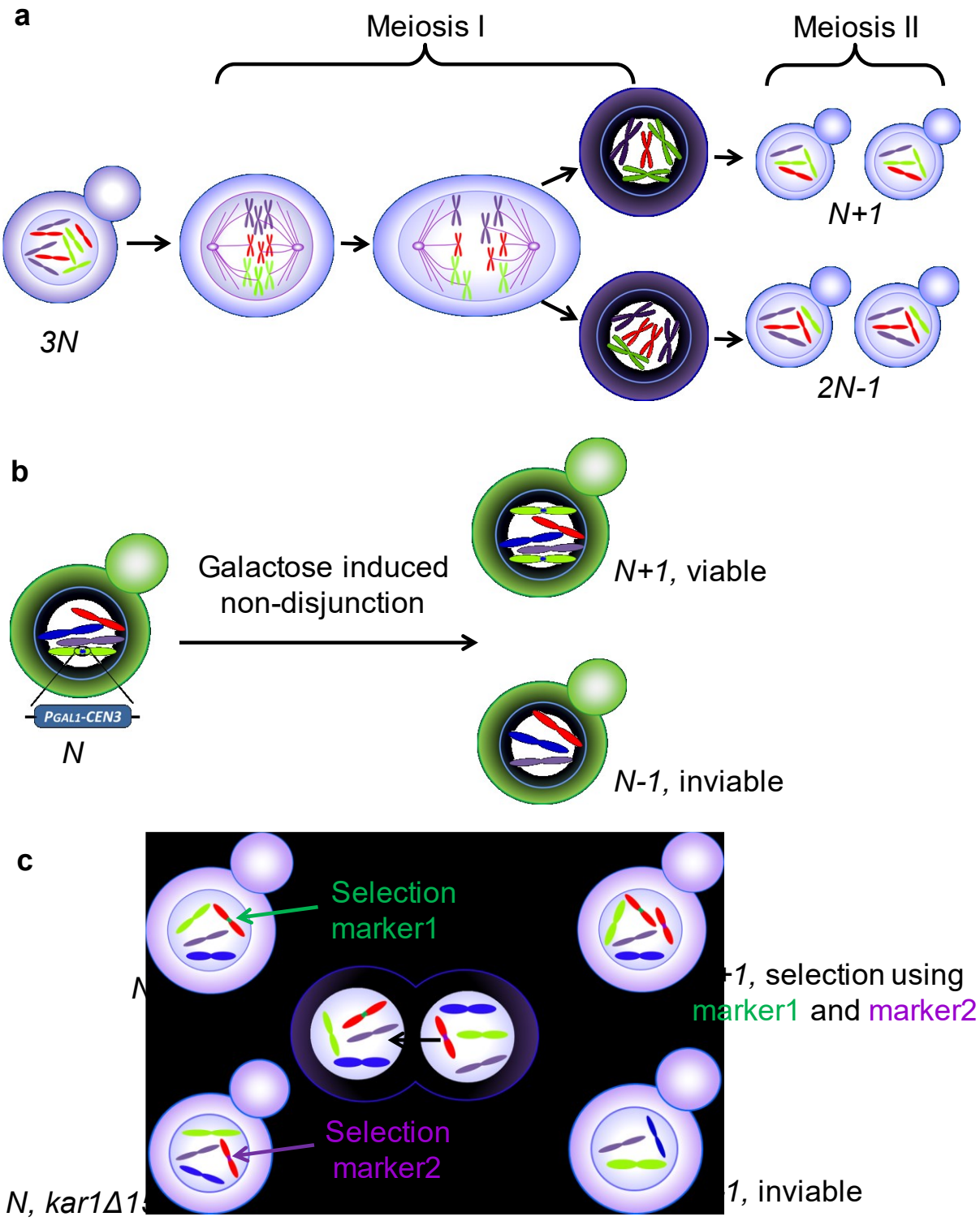

2.9.2 Figure 2: Characteristic examples of karyotyping methods.

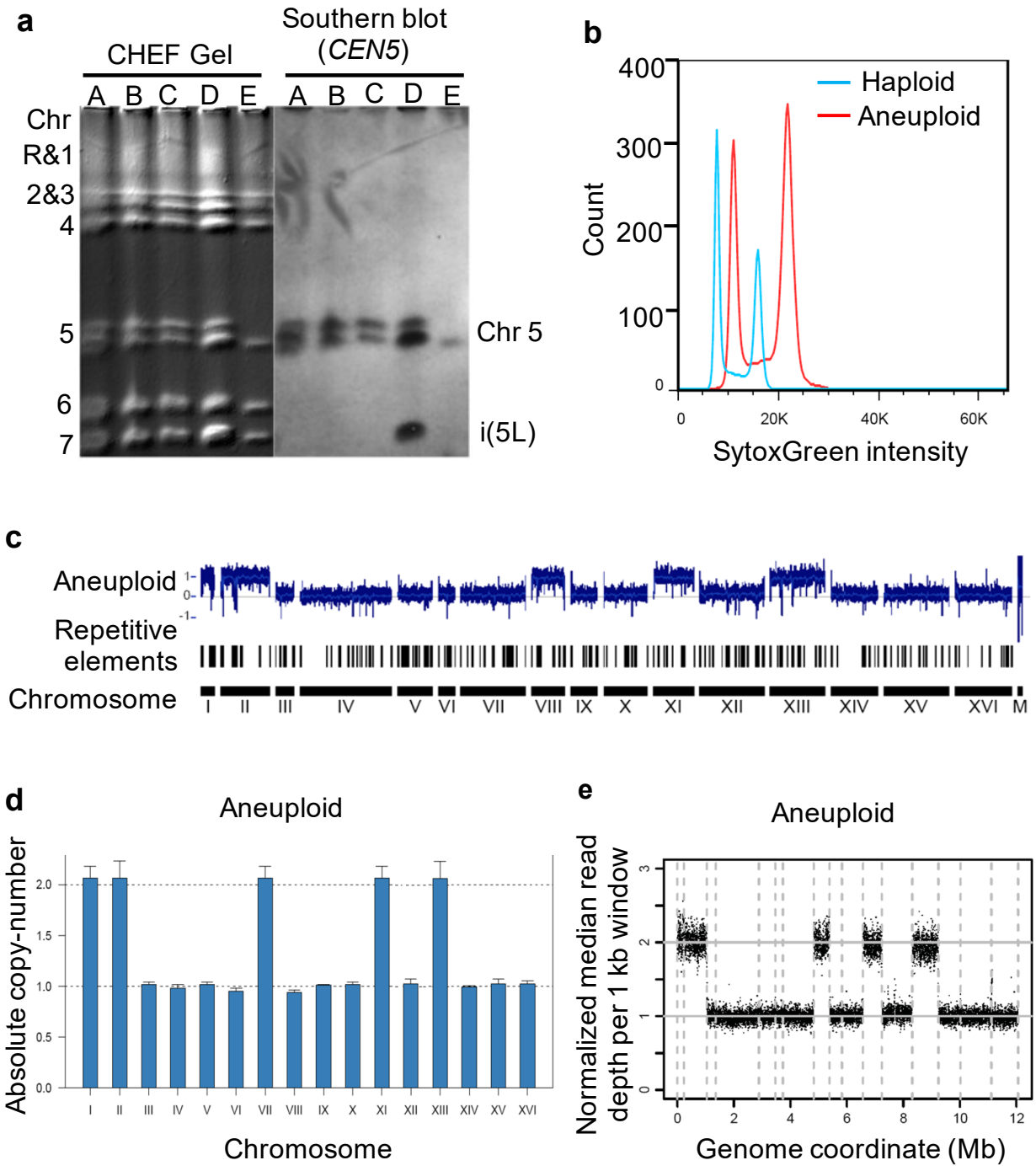

Table 2.10.1: Aneuploidy as an adaptive mechanism under different types of stress in yeast.

Type of stress	Species	Aneuploidy and implicated genes	Adaptive strategy	Reference
Therapeutic drug:				
Fluconazole (FLC)	*C. albicans*	i5: *ERG11, TAC1*	Resistance is acquired by up-regulation of *ERG11* encoding FLC target and *TAC1* encoding for a regulator of the drug efflux system.	(Selmecki, *et al.*, 2006, Coste, *et al.*, 2007, Selmecki, *et al.*, 2008)
	C. neoformins	Disomy I: *ERG11, AFR1*	Acquired resistance is attributed to up-regulation of *ERG11*, encodes drug target and AFR1, encodes major transporter of azoles.	(Sionov, *et al.*, 2010)
		Disomy IV: *SEY1, GLO3, GCS3*	Up-regulation of genes *SEY1, GLO3, GCS3* encoding a GTPase, linked with morphology and integrity of endoplasmic reticulum, a site of sterol synthesis.	(Ngamskulrungroj, *et al.*, 2012)
	C. glabrata	Chromosome M: *CDR1*	Elevated drug efflux by up-regulation of *CDR1.*	(Polakova, *et al.*, 2009)
Proteotoxic stress:				
Radicicol	*S. cerevisiae*	Disomy XV: *STI1, PDR5*	Resistance to radicicol is acquired by: improved protein	(Chen, *et al.*, 2012)

			folding by up-regulation of Hsp90 co-chaperone through increased expression of *STI1*. Over-expression of *PDR5* improves drug efflux system.	
DNA damage:				
4-NQO	*S. cerevisiae*	Disomy XIII: *ATR1*	Improved drug efflux by up-regulation of *ATR1* conferred resistance to 4-NQO.	(Pavelka, *et al.*, 2010)
Genetic perturbations:				
MYO1 deletion	*S. cerevisiae*	Trisomy and tetrasomy XVI: *RLM1, MKK2*	*RLM1*, *MKK2* mediated up-regulation of genes involved in cell wall biogenesis and bud neck constriction restoring cytokinesis.	(Rancati, *et al.*, 2008)
Deletion of *RPS 24A* and *RNR1* on Chr. V	*S. cerevisiae*	Disomy IX: *RPS24B* and *RNR3*	It is suggested that gain of chromosome IX might have been a result of a selection for growth advantage by increasing gene dosage of the paralogue of the deleted gene.	(Hughes, *et al.*, 2000)
Nutrient Limitations:				
Sulphate limitation	*S. cerevisiae*	Segmental gain of chromosome II: *SUL1*	Improved drug efflux by up-regulation of SulP anion transporter through elevated SUL1 level.	(Gresham, *et al.*, 2008)

Carbon source manipulation, l-sorbose/ d-arabinose	*C. albicans*	Monosomy V: *SOU1*	Monosomy of chromosome 5 activates SOU1 expression enabling l-sorbose.	(Rustchenko*, et al.*, 1994, Janbon*, et al.*, 1998)
High temperature	*S. cerevisiae*	Gain of chromosome III	---	(Yona*, et al.*, 2012)
High pH	*S. cerevisiae*	Gain of chromosome V	---	(Yona*, et al.*, 2012)

Chapter 3

Aneuploidy as a cause of impaired chromatin silencing and mating-type specification in budding yeast

The contents are adapted from:

Aneuploidy as a cause of impaired chromatin silencing and mating-type specification in budding yeast. Mulla WA, Seidel CW, Zhu J, Tsai HJ, Smith SE, Singh P, Bradford WD, McCroskey S, Nelliat AR, Conkright J, Peak A, Malanowski KE, Perera AG, Li R. eLife 2017.

3.1 Abstract

Aneuploidy and epigenetic alterations have long been associated with carcinogenesis, but it was unknown whether aneuploidy could disrupt the epigenetic states required for cellular differentiation. In this study, we found that ~3% of random aneuploid karyotypes in yeast disrupt the stable inheritance of silenced chromatin during cell proliferation. Karyotype analysis revealed that this phenotype was significantly correlated with gains of chromosomes III and X. Chromosome X disomy alone was sufficient to disrupt chromatin silencing and yeast mating-type identity as indicated by a lack of growth response to pheromone. The silencing defect was not limited to cryptic mating type loci and was associated with broad changes in histone modifications and chromatin localization of Sir2 histone deacetylase. The chromatin-silencing defect of disome X can be partially recapitulated by an extra copy of several genes on chromosome X. These results suggest that aneuploidy can directly cause epigenetic instability and disrupt cellular differentiation.

3.1 Introduction

Studies in unicellular eukaryotes, such as the budding yeast *Saccharomyces cerevisiae*, have provided valuable insights into the effects of aneuploidy on gene expression and corresponding cellular phenotypes because diverse aneuploid strains that differ only in chromosome stoichiometry, but not in DNA sequence, can be readily generated (Pfau and Amon 2012, Mulla, Zhu et al. 2014). In yeast, chromosome copy number variation leads to scaled changes in the transcriptome and proteome for most of the genes carried on the aneuploid chromosome, as well as expression level changes that vary significantly more than the scaled amount for 5-10% of total genes distributed throughout the genome (Torres, Sokolsky et al. 2007, Rancati, Pavelka et al. 2008, Pavelka, Rancati et al. 2010, Sheltzer, Torres et al. 2012). The widespread but mostly moderate gene expression changes caused by aneuploidy lead to quantitative alterations in cell growth under a wide range of environmental conditions. However, the existing yeast studies have not addressed whether aneuploidy has the potential to alter the stable epigenetic states correlated with cellular differentiation. This is in part because yeast cells lack complex developmental fates and yeast genome comprises mostly open chromatin accessible to the transcriptional machinery (Millar and Grunstein 2006).

Yeast cells, however, do have a few well-established regions of silenced chromatin, including the cryptic mating type loci *HML* and *HMR* on chromosome III, the *rDNA* repeats on chromosome XII, and subtelomeric regions (Buhler and Gasser 2009). In particular, chromatin silencing at *HML* and *HMR* is critical for the specification of the sexual identity of yeast, in the form of *a* or *α* mating type, which is stably inherited from generation to generation. The underlying epigenetic mechanism of mating type specification depends on

the recruitment of the Sir2 NAD-dependent histone deacetylase to *HM* loci through interactions with other Sir proteins (Sir1, 3, and 4) and several other accessory factors (Liou, Tanny et al. 2005, Kueng, Oppikofer et al. 2013, Behrouzi, Lu et al. 2016). Spreading of the Sir protein complex across this region of DNA leads to hypoacetylated histones and establishes stably silenced chromatin (Rusche, Kirchmaier et al. 2003).

In this study, we took advantage of the genetic tools available in yeast and used *HML* silencing as the primary readout to test whether aneuploidy can affect cell identity by disrupting heterochromatin chromatin assembly and maintenance. By inducing meiosis in triploid cells, we generated thousands of aneuploid colonies and screened them using an imaging-based assay to determine the frequency at which aneuploid karyotypes disrupted transcriptional silencing at *HML*. Using a battery of genomic, transcriptomic and cell biological analyses, we investigated the mechanisms by which aneuploidy caused defects in chromatin silencing and epigenetic inheritance.

3.2 Results

3.2.1 Diverse aneuploid karyotypes can cause chromatin desilencing

To investigate whether and at what frequency random chromosome stoichiometries could disrupt chromatin silencing, we started with a haploid yeast strain containing a yellow fluorescent protein (YFP) with a nuclear localization sequence under the *URA3* promoter, which was inserted into the silent *HML* locus. This *HML::YFP* reporter was shown previously to respond to transcriptional silencing in a Sir2, and 3-dependent manner, like the genes that normally reside at the silent mating type loci (Xu, Zawadzki et al. 2006). We converted the haploid strain carrying *HML::YFP* to a fully isogenic and homozygous

triploid strain by cycles of mating-type switching and mating (Figure 1 - figure supplement 1A) as previously described (Pavelka, Rancati et al. 2010). The resulting triploid strain, which exhibited complete silencing at the *HML* locus as indicated by the lack of YFP fluorescence (Figure 1B), were then sporulated and viable meiotic progenies were isolated through tetrad dissection. Previous studies showed that ~100% of the resulting colonies were aneuploid with random combinations of chromosome numbers, due to the segregation of 3 sets of homologous chromosomes during meiosis (Campbell, Doctor et al. 1981, Pavelka, Rancati et al. 2010, St Charles, Hamilton et al. 2010). Using fluorescence microscopy, we examined and identified individual colonies with defects in the silencing of YFP at the *HML* locus. Roughly 3% (98 out of 3418) of viable aneuploid spore colonies exhibited varying degrees of silencing defects. In contrast, we did not observe silencing defects in haploid meiotic progenies (n=100) obtained through sporulation of a diploid strain carrying the *HML::YFP* reporter as a control (data not shown).

To study how the imbalance of specific chromosomes alters chromatin silencing, we first determined which of the desilenced aneuploid strains had stable karyotypes, since most of the yeast aneuploids obtained through triploid meiosis are karyotypically unstable (Pavelka, Rancati et al. 2010). Using fluorescence-activated cell sorting (FACS) and qPCR karyotyping analyses, as previously described (Pavelka, Rancati et al. 2010), we identified 24 aneuploid strains with unique and stable karyotypes, each with gain or loss of multiple chromosomes compared to the basal ploidy – defined as the copy number possessed by most chromosomes (Table 1). In the desilenced strains, Chromosome (Chr) III, Chr X, Chr XII, and Chr XIII showed the most abundant copy number variation (more specifically, gain) (Figure 1C). In particular, Chr III and Chr X were significantly enriched as

chromosomes in gained aneuploid numbers in the desilenced aneuploid strains compared with a set of stable aneuploid strains of the same genetic background (S288c) that were isolated through triploid meiosis but not selected for silencing phenotype (Pavelka, Rancati et al. 2010) (Figure 1C).

We subsequently focused on the four aneuploid strains showing the most prominent defects in *HML* silencing for more in-depth analysis (Figure 1B, D). To exclude the possibility that the silencing defect was caused by spontaneously arising mutations rather than aneuploidy, all four aneuploid strains were subjected to whole-genome sequencing to compare with the parental euploid strains. This analysis revealed an absence of coding region mutations that were not already present in the parental euploid strains (see Materials and Methods).

Quantification of the mean fluorescence intensity for each of the four aneuploid populations showed a significant increase in YFP expression compared with the WT haploid control strains (Figure 1D). The extent of *HML::YFP* reporter desilencing in the aneuploid strains was comparable to or greater than that of the Δ*sir1* strain (Figure 1D). Interestingly, YFP expression was heterogeneous within each aneuploid population, and such heterogeneity was also observed in Δ*sir1* strain as reported previously (Xu, Zawadzki et al. 2006). To ensure the heterogeneous expression pattern of YFP^+ and YFP^- signals within the population was not due to the karyotypic variations, cells with 2x Chr III and 1x Chr X gain were sorted into two distinct subpopulations based on YFP fluorescent signal for further analysis, and qPCR karyotyping showed that both sub-populations retained the expected karyotype with gain of Chr III and X (Figure 1 - figure supplement 1B-D). To determine if this heterogeneity was due to the instability of the chromatin silencing state,

we performed time-lapse imaging of YFP expression over several cell divisions in aneuploid strains. We observed transitions between repression and derepression of the *HML* locus in proliferating cell lineages (Figure 1 - figure supplement 1E-G), which was never observed in haploid lineages (data not shown), suggesting that these aneuploid karyotypes disrupted the stable inheritance of the silenced chromatin.

We next used quantitative RT-PCR (qPCR) analysis to confirm the defective *HML* silencing observed by microscopy. This analysis revealed significant derepression of several genomic loci across different chromosomes that are normally silenced (Li, Mueller et al. 2006, Ellahi, Thurtle et al. 2015), including not only *YFP* at *HML* but also the subtelomeric genes *YFR057W, COS12, AAD15,* and *PAU4* and the *rDNA* region gene *NTS1-2* (Figure 1E). The observation of increased gene expression at all three genomic regions previously implicated in chromatin silencing (Talbert and Henikoff 2006) demonstrates that aneuploidy can affect global gene expression by altering the state of chromatin silencing, in addition to the previously shown effects related directly to changes in DNA copy number (Torres, Sokolsky et al. 2007, Rancati, Pavelka et al. 2008, Pavelka, Rancati et al. 2010, Sheltzer, Torres et al. 2012).

3.2.2 Chromosome X disomy is the simplest karyotype that disrupts chromatin silencing

Since each of the above strains had multiple aneuploid chromosomes, we performed segregation analysis to determine which chromosome aneuploidy was linked to the silencing phenotype. We treated two strains, one with gains in Chr III (2x), and X (III, III, X-gain) and the other with gains in Chr I, X, XII, and XIII (I, X, XII, XIII-gain), with

low concentrations of radicicol, an inhibitor of Hsp90, to induce chromosomal instability and karyotype changes (Chen, Bradford et al. 2012). We then isolated and karyotyped various aneuploid segregants from these strains (see methods) and analyzed silencing of the *HML::YFP* reporter. Analysis of the aneuploid segregants obtained from the aneuploid strain (III, III, X-gain) showed that the desilencing phenotype co-segregated with Chr X as the only gained chromosome (referred as disome X hereafter) (Figure 2A). Interestingly, the gain of one or two extra copies of Chr III, which carries the *HM* loci, did not affect *HML* silencing on its own. Furthermore, qPCR analysis revealed that two extra copies of Chr III did not cause transcriptional derepression of *HML*:*YFP*, subtelomeric genes, or *rDNA* regions (Figure 2B). However, gaining two copies of Chr III did exacerbate the silencing defect of disome X (Figure 2A). Disome X segregants independently obtained from the second aneuploid strain (I, X, XII, XIII-gain) also showed significant *HML* desilencing (Figure 2A). Conversely, a segregant from the above karyotype with extra copies of Chr I, XII, and XIII, but not Chr X, did not show a significant difference in *HML* silencing compared with the haploid control (Figure 2A). These observations establish a causal link between Chr X gain and *HML* desilencing.

To further test whether an acute gain of Chr X would be sufficient to cause *HML* desilencing, we induced Chr X disomy using a previously described conditional centromere strategy (Reid, Sunjevaric et al. 2008, Anders, Kudrna et al. 2009). In both WT haploid cells and aneuploid strains with two extra copies of Chr III, we integrated the *GAL1* promoter (P_{gal1}) into the region of Chr X directly adjacent to the consensus centromere sequences (P_{gal1}-*CEN-X*). Upon galactose addition, this *GAL1* promoter was activated to induce mitotic non-disjunction of Chr X, resulting in one viable progeny cell with an extra

copy of Chr X and an inviable one per cell division. For both the haploid and aneuploid strains that contained the P_{gal1}-*CEN-X* construct, growth in galactose resulted in a significant increase in YFP expression from *HML* compared with corresponding control strains, Chr X*::*P_{gal1}, in which P_{gal1} was integrated into Chr X at sites distant from the consensus centromere sequences (Figure 2C). This result further confirmed that gain of Chr X was sufficient to disrupt chromatin silencing at *HML*.

Because the heterogeneity in desilencing was similar between disomy X and *Δsir1*, we further combined disomy X and *Δsir1* to test whether these genetic lesions disrupt *HML* silencing through the same or different mechanisms. Notably, the fluorescence of the *HML::YFP* reporter in this double mutant was significantly higher ($p < 0.05$) than in either disome X or Δ*sir1* individually, suggesting an additive or synergistic effect between these genetic abnormalities on *HML* locus silencing (Figure 2D).

3.2.3 Disomy X impairs growth arrest in response to α-factor

MATa haploid yeast cells normally respond to the pheromone α-factor by switching from vegetative growth to a G1 cell cycle arrest. Desilencing at *HM* loci results in the expression of both *a*- and *α*- specific genes and the inability to respond to pheromones (Osborne, Dudoit et al. 2009). To test whether the effect of aneuploidy on silencing influences the pheromone-induced growth arrest, we treated WT haploid, *Δsir1* and disome X strains, all of the *a* mating type with the endogenous copy of the *HML* locus (non-YFP inserted), with α-factor for 90 min. FACS-based cell cycle analysis showed that, while WT haploid cells were fully arrested in the G1 phase, 23%±1.7% of *Δsir1* and 14%±1.5% of disome X cells remained in G2 (Figure 3A). We next applied filter discs saturated with α-

factor to a lawn of WT haploid, *Δsir1* and disome X *MATa* cells. The latter two strains showed significant reductions in pheromone sensitivity compared with the WT haploid population (Figure 3B). This demonstrates that the silencing defect of disome X impairs the ability of these aneuploid cells to undergo growth arrest in response to a paracrine factor.

3.2.4 Chromatin desilencing in disome X is associated with increased acetylation of H4K16 and reduced Sir2 enrichment across *HM* loci

Hypoacetylation of histone H4 at lysine 16 (H4K16) is essential for the establishment and maintenance of silencing at *HM* loci and subtelomeric genes (Katan-Khaykovich and Struhl 2005, Osborne, Dudoit et al. 2009). The deacetylation of H4K16 is carried out by Sir2, an NAD-dependent histone deacetylase that localizes to silenced chromatin (Thurtle and Rine 2014). To uncover whether the distribution of acetylated H4K16 (H4K16ac) and occupancy of Sir2 is affected in the disome X strain, we performed chromatin immunoprecipitation (ChIP) using anti-H4K16ac antibody in the haploid, aneuploid, and *Δsir1* strains, followed by qPCR using primer sets spanning *HML* and *HMR*. We observed significantly increased acetylation of H4K16 across both *HM* loci in disome X and *Δsir1* cells compared with WT haploid controls (Figure 4A-B). Similarly, we performed ChIP using anti-Sir2::HA antibody and found significantly reduced levels of Sir2 protein localized to both *HM* loci in the disome X and *Δsir1* strains, compared to WT haploid control (Figure 4C-D). These results suggest that the defective silencing of *HM* loci in disome X cells may result from a reduction in chromatin-localized Sir proteins, such as Sir2, and the corresponding increased acetylation of H4K16 at these sites.

3.2.5 Loss of *HML* silencing in disome X cells is associated with a dispersed distribution of Sir2 and altered chromatin positioning

The silencing of the *HM* loci and subtelomeric regions is associated with characteristic distributions for both Sir2 protein and the chromatin regions within the nucleus (Andrulis, Neiman et al. 1998, Taddei, Van Houwe et al. 2009). To further understand the mechanism by which disomy X affects chromatin silencing, we examined the localization of endogenous Sir2, tagged at the genomic locus with mTurquoise (mTurq), and observed that the Sir2-mTurq signal was more diffuse in disome X compared with WT haploid cells (Figure 5A). We quantified this difference by calculating the coefficient of variation (CV; standard deviation/mean) of fluorescence pixel intensities within the sum projection of each cell (Figure 5B). The CV was significantly reduced for Sir2-mTurq fluorescence in disomy X compared with WT haploid populations ($p < 0.001$, two-tailed t-test), particularly in the 35% of aneuploid cells that had a significantly higher ($p < 0.01$) mean expression of YFP from the *HML* locus than the haploid control. The more dispersed Sir2 distribution in disome X cells is consistent with the reduced concentration of Sir2 in silenced chromatin regions (Figure 4C-D). This analysis was designed to quantitatively reflect the difference in the "sharpness" of Sir2 localization while accounting for the difference in overall fluorescence level in each cell (Figure 5 - figure supplement 1A-C).

The positioning of chromatin relative to the nuclear envelope is also important for silencing (Bystricky, Van Attikum et al. 2009, Mekhail and Moazed 2010). To address whether the normal perinuclear positioning of silenced chromatin was disrupted in disome X cells, we introduced the *LacO* array into the *HML* locus and expressed LacI-GFP to

obsereve the *LacO* array-marked site in the nucleus, demarcated with the nuclear envelope (NE) marker Nup60-mCherry. We defined three concentric nuclear zones of equal area - NE (Zone 1), medial (zone 2), and central (zone 3) regions and determined the percentage of cells with the GFP puncta, corresponding to *HML*, in each zone. We observed a significant ($p < 0.05$) reduction in the percentage of disomy X cells with their *HML* locus attached to the NE (zone 1) compared with the WT haploid strain. This was accompanied by a corresponding increase in the percentage of cells with *HML* located in the central nuclear zone (zone 3), suggesting that the silencing defect of the disome X strain is associated with altered chromatin positioning in the nucleus (Figure 5C).

3.2.6 Gain of Chromosome X alters subtelomeric gene expression through changes in H3K4me3 and H3K79me3

To determine if disomy X leads to a genome-wide alteration of histone modification, we assessed two histone modifications associated with active chromatin, trimethylation of histone H3 at either Lysine 4 (H3K4me3) or Lysine 79 (H3K79me3), by performing chromatin immunoprecipitation followed by next-generation sequencing (ChIP-seq). In parallel, we analyzed a portion of the same experimental cultures by RNA sequencing (RNA-seq) to correlate genome-wide changes in histone modifications with the transcriptional output. The number of methylated genes (~60% of total *S. cerevisiae* genes) in the disome X and WT haploid strains was not significantly different (Table 2). Consistent with previous reports (Pokholok, Harbison et al. 2005, Guillemette, Drogaris et al. 2011, Takahashi, Schulze et al. 2011), both strains showed an overall positive

correlation between gene expression and H3K4me3 enrichment, but not H3K79me3 (Figure 6 – figure supplement 1A).

To compare the epigenetic and transcriptional changes in aneuploid cells, we plotted the difference in H3K4me3 enrichment between disome X and WT haploid strains against the fold change in gene expression for each of the 3502 genes (~57% of the total genes in the yeast genome, Table 2) that were expressed with detectable H3K4me3 marks in both strains. At the genome-wide level, we found no correlation between an increased enrichment of H3K4me3 modifications and increased gene expression in disome X cells compared with the haploid control (Figure 6A). Likewise, there was no difference in gene expression between disome X and haploid populations for sets of genes that had H3K4me3 modifications only in one strain or the other (Figure 6 – figure supplement 1B and C). However, most of the subtelomeric genes that were expressed and modified in both strains (Table 2) were significantly enriched (p-value= 2.5×10^{-8}, Fisher's exact test) for H3K4me3 modifications and had higher expression levels in disome X cells compared with the haploid control (Figure 6A).

The H3K79me3 histone mark has previously been implicated in the regulation of subtelomeric silencing by modulating the binding of Sir proteins to these chromatin regions. In our ChIP- and RNA- seq experiments, three subtelomeric genes, *COS12, IMD2,* and *YIR042C,* showed significantly increased RNA expression levels and enriched H3K4me3 and H3K79me3 modifications in disome X cells compared with WT (Figure 6C-D). Notably, *COS12* was previously identified as a target of H3K79me3-regulated silencing (Takahashi, Schulze et al. 2011). On the genome-wide level or in subsets of genes carrying H3K79me only in one or the other strain, however, we observed no correlation

between transcription levels and this epigenetic mark in disome X cells relative to WT (Figure 6B, Figure 6 – figure supplement 1D-E and Table 2).

3.2.7 The *HML* silencing defect results from increased copy number of at least four genes on Chr X

To identify the genetic components that contribute to the silencing defect caused by an extra copy of Chr X, we used the *HML::YFP* reporter and fluorescence microscopy to screen the effect of an increased copy number of each of the 304 genes located on Chr X, for loss of YFP silencing in the disome III background as a means to sensitize the screen. We took advantage of the yeast MOBY library, in which each gene, with its endogenous promoter, is carried on a low-copy (centromeric) plasmid (Ho, Magtanong et al. 2009). The fifteen Chr X genes with top-ranked silencing defect were further verified by transforming the centromeric plasmid into a WT haploid strain (Table 3). Because cells can maintain up to four copies of centromeric plasmids, we next integrated a single extra copy of each of the top ten candidate genes into a WT haploid genome, but we found that none of these individual genes significantly disrupted silencing when present at this level (data not shown).

Two genes, *RPL39* and *RPS14B,* encoding ribosomal proteins, were among those with the strongest silencing defects when expressed on a centromeric plasmid. Since previous studies showed that overexpression of a ribosomal protein-encoding gene, *RPL32,* impaired silencing (Singer, Kahana et al. 1998), we tested the effect of combining single extra copies, via integration, of *RPL39* and *RPS14B* together in the haploid genome; however, this combination did not alter silencing of the *HML::YFP* reporter (Figure 7A,

B). Previous studies also showed that silencing is affected by one other top candidates from our MOBY library screen *ASF1*, which encodes a nucleosome assembly factor (Singer, Kahana et al. 1998, Smith, Caputo et al. 1999). Integration of *ASF1* together with *DPB11*, a top hit in our screen but not previously known to affect silencing, into the haploid genome also showed no effect on silencing (Figure 7A, B). However, when we combined all four genes tested above (*RPL39*, *RPS14B, ASF1, and DPB11*) by integrating them into the haploid genome, significant *HML* desilencing was observed compared to the haploid control, although the effect was not as strong as that in disome X cells (Figure 7A, B). These results suggest that the disomy X-induced desilencing is complex and requires the combined effects of at least four Chr X-linked genes.

3.4 Summary:

Our imaging-based analysis of thousands of freshly-produced aneuploid yeast colonies demonstrated that roughly 3% of random aneuploid karyotypes disrupt transcriptional silencing at the *HML* locus, indicating that aneuploidy can impact gene expression to an extent far greater than the effects resulting from direct gene-dosage changes. We identified specific karyotypic features associated with the silencing defect, with the simplest being gain of Chr X, which is sufficient to destabilize the epigenetic state and alter cellular responses to a relevant physiological factor (α-factor). Furthermore, the loss of silencing at the *HM* loci on Chr III and transcriptional derepression at subtelomeric regions on different chromosomes induced by Chr X disomy correlated with changes in the histone modification landscape, including increased H4K16 acetylation, and H3K4 and H3K79 trimethylation. Moreover, the silencing defect of disome X cells was associated

with perturbed chromatin localization within the nucleus. The genetic basis of disome X-induced desilencing is complex, requiring at least four Chr X genes. Taken together, our results provide the evidence that aneuploidy can be a direct genetic cause of epigenetic dysregulation.

3.4 Main Figure legends

Figure 3.4.1: Aneuploid yeast strains show defective silencing at *HML*, subtelomeric, and *rDNA* chromatin regions.

(A) The design of a microscopy-based screen to isolate karyotypically stable aneuploid strains, generated by inducing triploid meiosis, that exhibit defective silencing of the *HML* locus.

(B) Representative fluorescence images show *HML::YFP* reporter expression in euploid and aneuploid cells of various karyotypes, as indicated. YFP expression from the *HML* locus is not detectable in the parental haploid, diploid and triploid strains; YFP fluorescence is heterogeneous within *Δsir1* and aneuploid cell populations suggests defective silencing at the *HML* locus. Scale bar, 4 μm.

(C) The bar plot shows the number of times each of the sixteen yeast chromosomes was found to be aneuploid (chromosome number different from the basal ploidy) in 24 strains with defective silencing. Aneuploidies of Chr III and Chr X are significantly overrepresented in strains with defective silencing compared with other 38 stable aneuploids isolated by the same method (Pavelka, Rancati et al. 2010). *$p < 0.05$ for Chr III and Chr X; $p = 0.09$ for Chr XII calculated using an exact binomial test.

(D) The box plot shows mean YFP intensities, determined by microscopy as in Figure 1B, for 175 individual cells per strain. The karyotype of each aneuploid strain is indicated; WT and *Δsir1* cells are haploid. The box spans the first through third quartile values, the line inside each box indicates the median, the solid black square designates the mean, and the whiskers mark the 90/10 percentile range. *$p < 0.01$, **$p < 0.001$, ***$p < 0.0001$ compared with WT haploid; calculated using a Mann–Whitney U test.

(E) The bar plot depicts the expression, measured by quantitative RT-PCR, of several normally silenced genes: YFP inserted into the endogenous *HML* locus; subtelomeric genes *YFR057W (Chr III), COS12 (Chr XII), AAD15 (Chr XV), and PAU4 (Chr XII); and rDNA gene NTS1-2 (Chr XII).* Transcriptional levels are plotted as fold expression relative to the WT haploid strain. Error bars represent the standard deviation (SD) of three biological replicates. *$p < 0.05$, **$p < 0.01$, ***$p < 0.005$ compared with WT haploid; calculated using a two-tailed t-test.

Figure 3.4.2: Gain of Chr X is sufficient to disrupt silencing.

(A) The box plot shows mean YFP intensities, determined by microscopy of 125 individual cells for each of the following strains: WT haploid, *Δsir1*, and two parental aneuploid strains (Gain of III, III, X and Gain of I, X, XII, XIII) and their segregants (Gain of III; Gain of III, III; and Gain of I, XII, XIII). The box spans the first through third quartile values, the line inside each box indicates the median, the solid black square designates the mean, and the whiskers mark the 90/10 percentile range. *$p < 0.01$, **$p < 0.001$, ***$p < 0.0001$ compared with WT haploid unless indicated by brackets; calculated using a Mann–Whitney U test.

(B) The bar plot depicts the expression, measured by quantitative RT-PCR, of several normally silenced genes in haploid and aneuploid cells with two extra copies of Chr III. These genes are YFP inserted into the endogenous *HML* locus; subtelomeric genes *YFR057W (Chr III), COS12 (Chr XII), AAD15 (Chr XV), and PAU4 (Chr XII); and rDNA gene NTS1-2 (Chr XII).* Transcription levels are plotted as fold expression relative to the WT haploid strain and not significantly different in Gain III, III strain compared to WT haploid ($p < 0.05$, calculated using a two-tailed t-test). Error bars represent SD of three biological

replicates.

(C) The box plots show mean YFP intensities, determined by microscopy of 125 individual cells for each of the indicated WT haploid or aneuploid strains. The *GAL1* promoter (*Pgal1*) was integrated into Chr X either directly adjacent to (*Pgal1-CEN-X*) or far from (Chr X*::Pgal1*) consensus centromere sequences. The box plot presentation and statistical analysis are performed as described in Figure 2A.

(D) The box plots show mean YFP intensities, determined by microscopy of 125 individual cells for each of the following strains: WT haploid, *Δsir1*, disome X/*SIR1* and disome X/*Δsir1* double mutant. The box plot presentation and statistical analysis are performed as described in Figure 2A.

Figure 3.4.3: Cells with a gain of Chromosome X show abnormal growth arrest in response to α-factor.

(A) The plots show FACS-based DNA content analysis, indicating cell cycle stage, in *MATa* WT haploid, *Δsir1*, and disome X strains. Left panels represent untreated cells; right panels represent strains treated with 2 µg/ml α-factor for 90 min. Peaks overlapping with the red dotted line represent cells in the G1 phase with a haploid genome content (1N). Peaks overlapping with the blue dotted line represent cells in the G2 phase with a diploid genome content (2N). Percentages are the fraction of total cells in G2, ± SD. *$p < 0.001$ compared with WT haploid; calculated using a two-tailed t-test.

(B) Images depict a pheromone sensitivity assay conducted by applying filter discs carrying α-factor (15 µl of 2 µg/ml) to lawns of WT haploid, *Δsir1*, or disome X *MATa* strains. The images shown were used to calculate the size of the zone devoid of cell growth (the region

between the rim of the disc and the dashed circle); these areas, indicative of cellular sensitivity to α-factor, were normalized to the WT haploid strain and plotted. The plot shows the mean and SD from three replicates per strain. *$p < 0.001$ compared with WT haploid; calculated using a two-tailed t-test.

Figure 3.4.4: *HM* desilencing in disome X cells correlates with increased H4K16 acetylation and reduced Sir2 enrichment across *HM* loci.

(A-B) Bottom: The plots show levels of H4K16 acetylation across the *HML* **(A)** and *HMR* **(B)** loci in disome X and *Δsir1* strains relative to WT haploid cells, determined using anti-H4K16ac chromatin immunoprecipitation (ChIP) followed by quantitative RT-PCR (qPCR) analysis. Top: Schematics of the *HM* loci indicate the genomic positioning of primer sets A to F used for qPCR. Plots show the mean and SD from three biological replicates. *$p < 0.05$, **$p < 0.01$, ***$p < 0.005$ calculated using two-tailed t-test and indicate statistically significant difference in H4K16 acetylation level at corresponding genomic locations in *Δsir1* and disome X strains compared to WT haploid.

(C-D) The plots indicate Sir2 occupancy across the *HML* **(C)** and *HMR* **(D)** loci in disome X and *Δsir1* strains relative to WT haploid cells, determined using anti-Sir2::HA ChIP followed by qPCR analysis with the same primer sets depicted in **(A)** and **(B)** for **(C)** and **(D)**, respectively. Plots show the mean and SD from three biological replicates. *$p < 0.01$, **$p < 0.005$ compared with WT haploid; calculated using t-test and indicate a statistically significant difference in Sir2 occupancy at corresponding genomic locations across *HM* loci in *Δsir1* and disome X strains compared to WT haploid.

Figure 3.4.5: Disome X cells display abnormal Sir2 protein localizations and lack proper perinuclear positioning of silenced chromatin region.

(A) Representative fluorescent images are shown for Sir2-mTurq and the *HML::YFP* reporter in WT haploid and disome X strains. White boxes in the top panels display magnified images (insets) of representative Sir2 foci. Scale bar, 4 μm.

(B) The scatter plots show, for each WT haploid or disome X cell, the coefficient of variation (CV) of Sir2-mTurq fluorescence plotted against the mean YFP pixel intensity. The CV was calculated as the ratio of the standard deviation to the mean pixel intensity of Sir2-mTurq fluorescence over the total area of the sum projection of each cell. The CV in the disome X strain is significantly reduced compared with haploid cells ($p < 0.001$, one-tailed t-test), indicating a more diffusive distribution of Sir2 in aneuploid cells. Additionally, 35% of disome X cells (determined using Tukey's outlier test on the WT strain) have significantly higher ($p < 0.01$) mean YFP intensities than the WT haploid cell population; these disome X cells also show significantly ($p < 0.05$) reduced CV compared with haploid controls.

(C) Left: Representative images show the position of the *HML* locus, tagged with *LacO* arrays and bound by LacI-GFP, relative to the nuclear envelope (NE), marked by Nup60-mCherry. Top right: The illustration shows the three concentric zones of the equal area used to map the location of the *HML* locus. Bottom right: The bar graph shows the percentage of WT haploid or disome X cells with GFP puncta located in each of the three zones (n = 100 cells per strain). Confidence values (p) are shown for a χ^2 analysis comparing random (33% in each zone) and test distributions. *: Value significantly differs from a random distribution ($p < 0.005$, Chi-square test for independence). Scale bar, 1 μm.

Figure 3.4.6: Genome-wide analysis shows that disome X cells upregulate histone modifications and transcription of typically silenced genes.

(A-B) Gene expression changes determined by RNA-seq are plotted on the X-axis as log2 fold change (disome X/WT haploid), and H3K4me3 **(A)** and H3K79me3 **(B)** histone modification enrichments determined by ChIP-seq are plotted on the Y-axis as the difference in Z-scores (disome X - WT haploid), with each dot representing an individual gene. Genes that were expressed (RPKM > 1) and enriched for a given histone modification in both haploid and disome X strains were included in this analysis and categorized into four groups: (I) Genome-wide, representing all of the included genes (grey dots); (II and III) Subsets of genes from category I that were significantly (1.5- fold change, $p < 0.01$) upregulated (blue dots) or down-regulated (green dots) in disome X cells compared with haploid controls; and (IV) subtelomeric genes (red dots). Note that identities of subtelomeric genes in A and B are different because the genes with occupancy of the two histone markers (K4me and K79me) were not the same and hence are at different points along the x-axis of A and B. More detailed information about the genes in these categories is listed in **Table 2**.

(C) Transcriptional levels of *COS12* (Chr XII)*, IMD2* (Chr VIII)*,* and *YIR042C* (Chr IX) genes were measured by RNA-seq and plotted as fold change (disome X/WT haploid). Each bar depicts the mean and SD of three biological replicates. *$p < 0.001$ compared with WT haploid; calculated using two-tailed t-test.

(D) Enrichment profiles of H3K4me3 and H3K79me3 were determined by ChIP-seq and plotted as reads per million per nucleotide (RPM) for the indicated gene ORFs (black arrows), with 500 bp of flanking sequence on both sides. Each plot shows the enrichment

profiles for two biological replicates per WT haploid or disome X strain. Both epigenetic marks are enriched at all three genomic loci in disome X cells compared with the haploid controls.

Figure 3.4.7: The combined increase in copy number of at least four genes on Chr X causes *HML* silencing defects.

(A) Representative images of YFP fluorescence from the *HML::YFP* reporter in *Δsir1*, disome X, and WT haploid cells with a single extra copy of the indicated genes, where relevant. Scale bar, 4 μm.

(B) The box plot shows the mean YFP intensity of 125 cells for each strain shown in Fig. 7A. The box spans the first through third quartile values, the line inside each box indicates the median, the solid black square designates the mean, and the whiskers mark the 90/10 percentile range. *$p < 0.01$, **$p < 0.001$, ***$p < 0.0001$ compared with WT haploid; calculated using a Mann–Whitney U test.

3.5 Supplementary Figure legends

Figure 3.5.1 – figure supplement 1.

(A) A schematic representation of the genetic manipulations used to generate isogenic diploid and triploid strains from the parental WT haploid strain, which has nuclear localization sequence-tagged YFP inserted into the *HML* locus.

(B) FACS sorting of YFP^- vs YFP^+ cells from the strain with 2x Chr III and 1x Chr X gain. Red and yellow line outlines the population of YFP^- and YFP^+ cells sorted for the qPCR analysis in C and D, respectively.

(C-D) qPCR karyotyping of YFP^- **(C)** and YFP^+ **(D)** cell population sorted from the strain with 2x Chr III and 1x Chr X gain. Chromosome copy numbers of sixteen yeast chromosomes are plotted as mean and SD of three technical replicates.

(E-G) Confocal images of YFP fluorescence, taken at the indicated time points during time-lapse imaging, show transitions between repression and derepression of the *HML* locus in proliferating lineages of aneuploid yeast cells with the following karyotypes: **(E)** Gain of III, III, X; **(F)** Loss of I, V, VII, VIII, XI (basal ploidy, 2N); and **(G)** Gain of I, X, XII, XIII. Arrows point to mother cells that switched from the silenced to the desilenced state. The circle outlines the boundary of the cell. Scale bar, 4 μm.

Figure 3.5.5 – figure supplement 1.

(A-B) Western blot analysis of total Sir2 protein by using anti-Sir2 and anti-α-PGK (loading control) antibodies for the following strains: WT haploid, *Δsir1*, disome X, and *Δsir2/SIR2.* The total Sir2 protein levels were quantified using densitometric analysis, normalized to the WT haploid strain and plotted in **(B)**.

(C) The box plot shows mean Sir2-mTurq intensities, determined by microscopy of 68 individual cells for WT haploid and disome X strains. The box spans the first through third quartile values, the line inside each box indicates the median, the solid black square designates the mean, and the whiskers mark the 90/10 percentile range. *$p < 0.001$ compared with WT haploid; calculated using a Mann–Whitney U test.

(D) The box plots show mean YFP intensities, determined by microscopy of 100 individual cells for each of the following strains: WT haploid, *Δsir1*, disome X and *Δsir2/SIR2*, all with YFP inserted into *HML*. The box plot presentation and statistical analysis are performed as described in **(C);** *$p < 0.01$, **$p < 0.001$.

Figure 3.5.6 – figure supplement 1.

(A) Expression levels determined by RNA-seq experiments are plotted as log10 of the RPKM values on the X-axis, and H3K4me3 enrichment determined by ChIP-seq analysis is plotted as log10 of the Z-scores on the Y-axis for individual genes in disome X (red) and WT haploid (green) strains.

(B-E) The violin plots show gene expression levels, plotted as log2 of the RPKM values, in disome X and WT haploid strains for individual genes carrying: **(B)** H3K4me3 enrichment in WT haploid but not disome X cells; **(C)** H3K4me3 enrichment in disome X but not haploid cells; **(D)** H3K79me3 enrichment in haploid but not disome X cells; and **(E)** H3K79me3 enrichment in disome X but not haploid cells. In these plots, the width of the violin shape at a given log2(RPKM) value indicates the number of genes expressed at that level. The white dot represents the geometric mean RPKM value for all the genes, and the thick and thin lines are box plots that show the first and third quartiles and 1.5 times interquartile ranges (IQR), respectively.

3.6 Table Legends

Table 3.6.1: The karyotypes of stable aneuploid strains that exhibit defective silencing of YFP at the *HML* locus obtained from a microscopy-based screen are listed.

Table 3.6.2: The number of genes plotted for each category in **Figure 6A-B** and **Figure 6 – figure supplement 1** is listed.

Table 3.6.3: A list of fifteen Chr X genes that cause the strongest silencing defects as a result of increased copy number. Genes leading to the loss of *HML::YFP* silencing when copy number is increased are listed with a functional description and a desilencing score. The desilencing score was calculated as the average YFP intensity in WT haploid strains carrying individual candidate genes on a low-copy (centromeric) plasmid, relative to the average YFP fluorescence in the disome X strain. Average YFP intensities were calculated using 3 biological replicates per strain.

Table 3.6.4. List of yeast strains used in this study, and not listed in **table 1.**

Table 3.6.5. List of plasmids used in this study.

3.7 Main Figures

3.7.1 Figure 1:

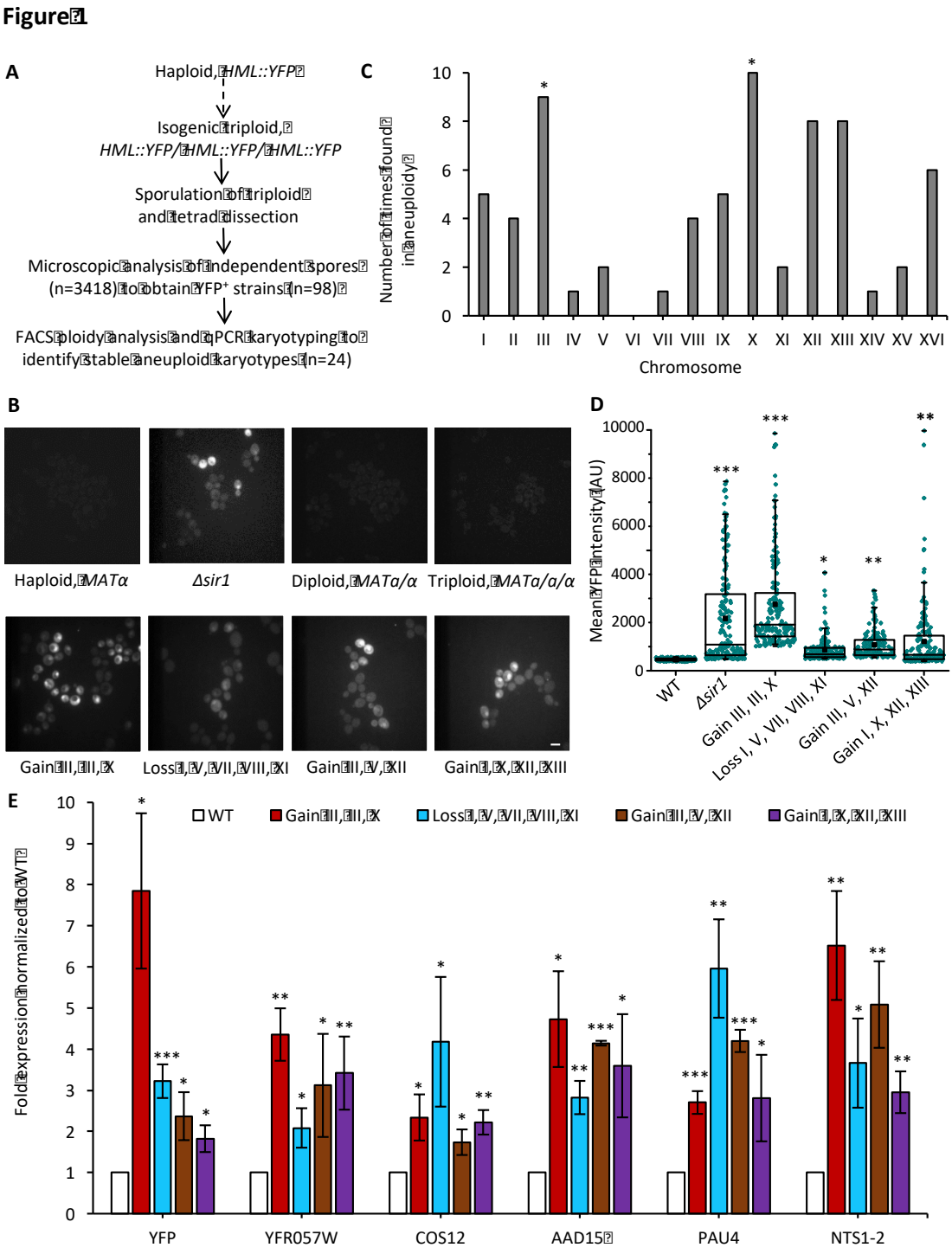

3.7.2 Figure 2:

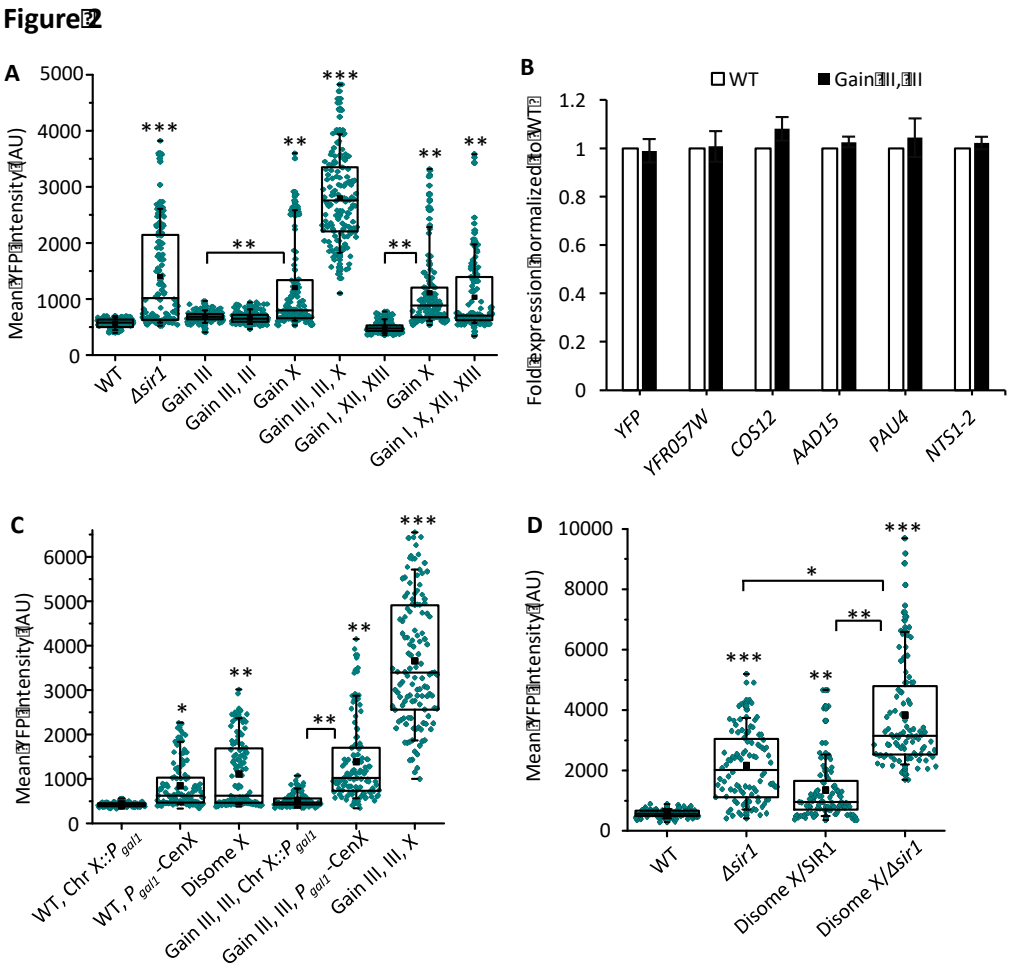
Figure 2
A
Mean YFP Intensity (AU)
5000
4000
3000
2000
1000
0
***
**
**
***
**
**
WT
Δsir1
Gain III
Gain III, III
Gain X
Gain III, III, X
Gain I, XII, XIII
Gain X
Gain I, X, XII, XIII
B
WT
Gain III, III
Fold expression normalized to WT
1.2
1
0.8
0.6
0.4
0.2
0
YFP
YFR057W
COS12
AAD15
PAU4
NTS1-2
C
Mean YFP Intensity (AU)
6000
5000
4000
3000
2000
1000
0
*
**
**
**
***
WT, Chr X::P gal1
WT, P gal1-CenX
Disome X
Gain III, III, Chr X::P gal1
Gain III, III, P gal1-CenX
Gain III, III, X
D
Mean YFP Intensity (AU)
10000
8000
6000
4000
2000
0
*
**
***
**
***
WT
Δsir1
Disome X/SIR1
Disome X/Δsir1

3.7.2 Figure 3:

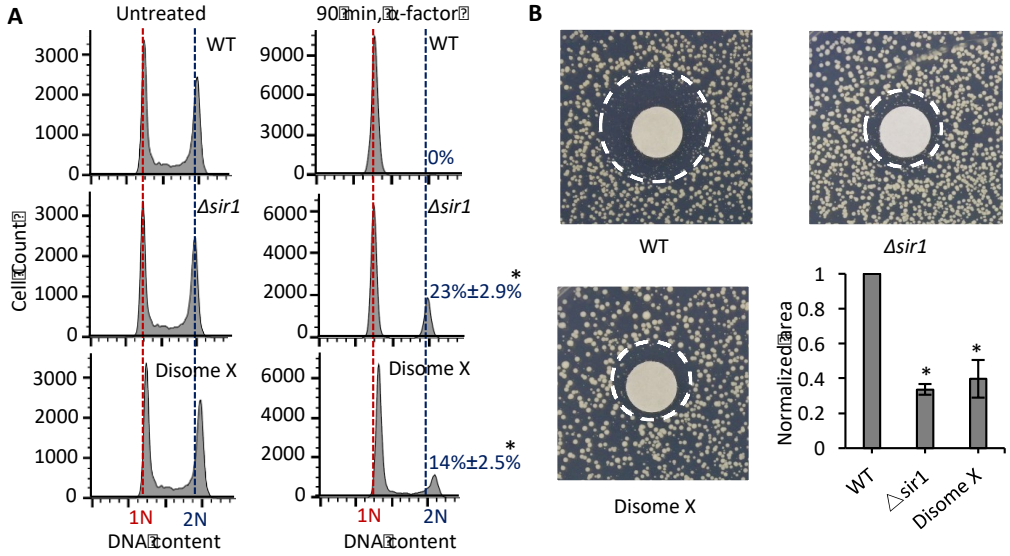
Figure 3
A
Untreated
90 min, α-factor
WT
Δsir1
Disome X
Cell Count
3000
2000
1000
0
9000
6000
4000
0%
23%±2.9%
14%±2.5%
*
1N
2N
DNA content
B
WT
Δsir1
Disome X
Normalized area
1
0.8
0.6
0.4
0.2
△sir1

3.7.4 Figure 4:

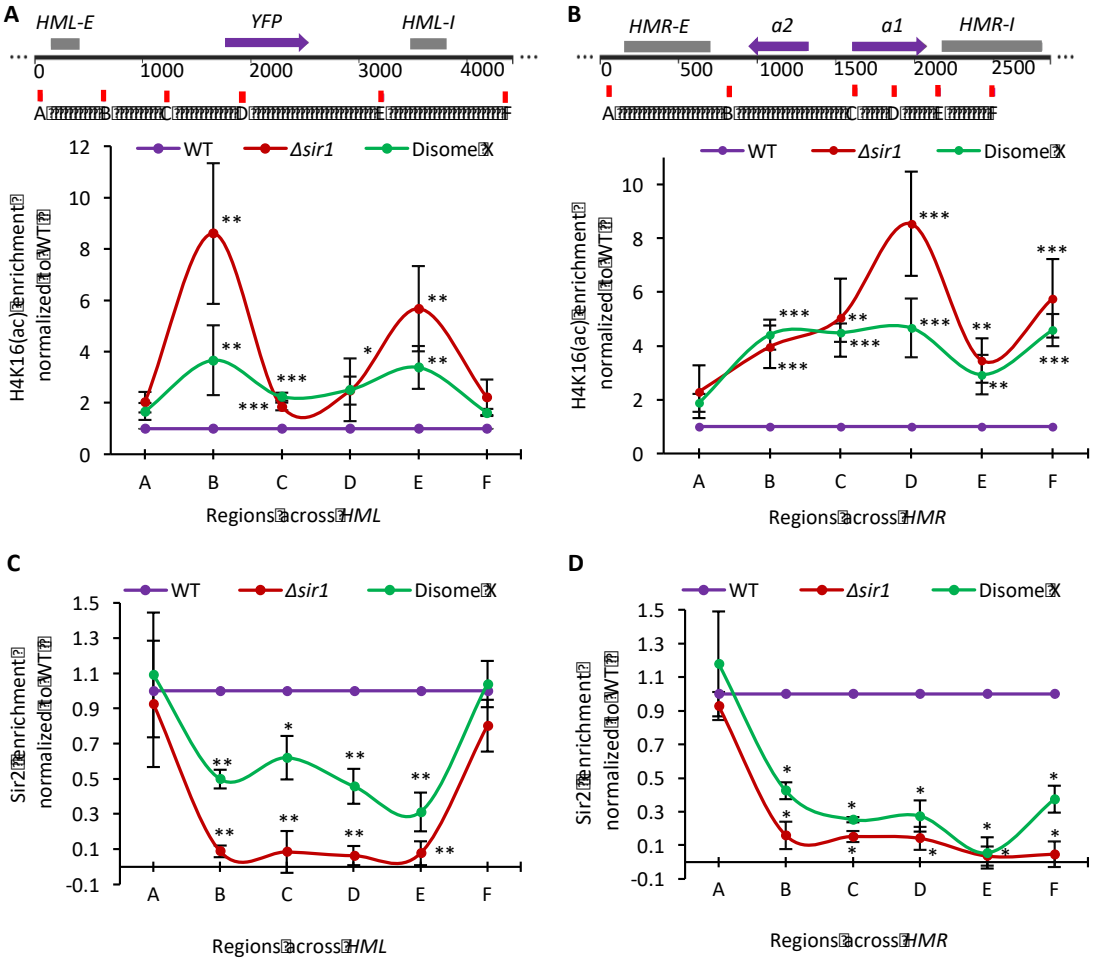
A
HML-E
YFP
HML-I
0
1000
2000
3000
4000
A
B
C
D
E
F
WT
Δsir1
Disome
H4K16(ac) enrichment normalized to WT
Regions across HML
B
HMR-E
α2
α1
HMR-I
0
500
1000
1500
2000
2500
Regions across HMR
C
Sir2 enrichment normalized to WT
Regions across HML
D
Regions across HMR

3.7.5 Figure 5:

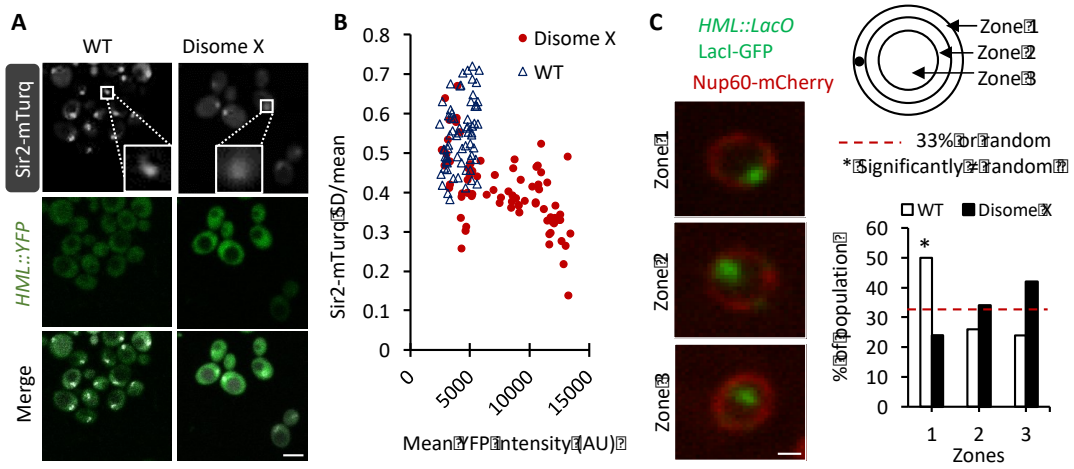
A
WT
Disome X
Sir2-mTurq
HML::YFP
Merge
B
Disome X
WT
Sir2-mTurq 5D/mean
Mean YFP Intensity (AU)
C
HML::LacO
LacI-GFP
Nup60-mCherry
Zone 1
Zone 2
Zone 3
33% or random
*Significantly ≠ random
WT
Disome X
% of population
Zones

3.7.6 Figure 6:

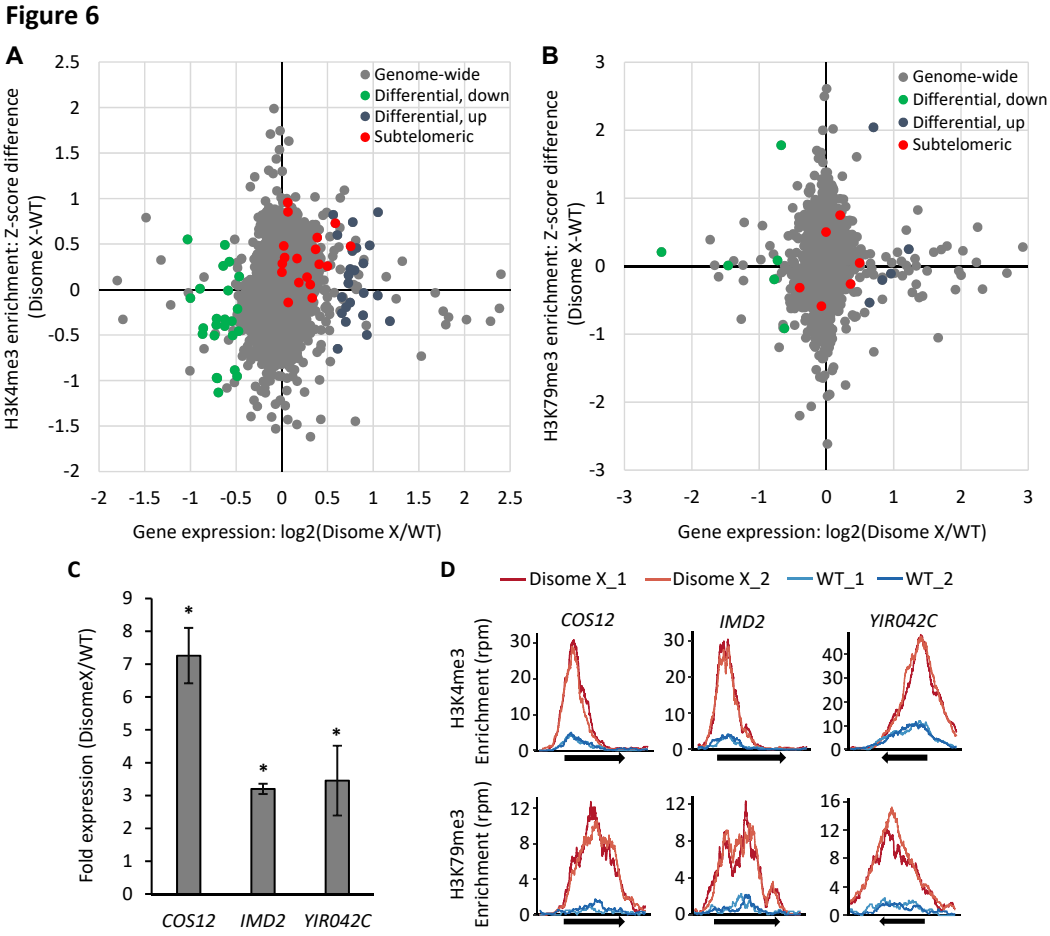
Figure 6
A
B
Genome-wide
Differential, down
Differential, up
Subtelomeric
H3K4me3 enrichment: Z-score difference (Disome X-WT)
H3K79me3 enrichment: Z-score difference (Disome X-WT)
Gene expression: log2(Disome X/WT)
C
Fold expression (DisomeX/WT)
COS12
IMD2
YIR042C
D
Disome X_1
Disome X_2
WT_1
WT_2
H3K4me3 Enrichment (rpm)
H3K79me3 Enrichment (rpm)

3.7.7 Figure 7:

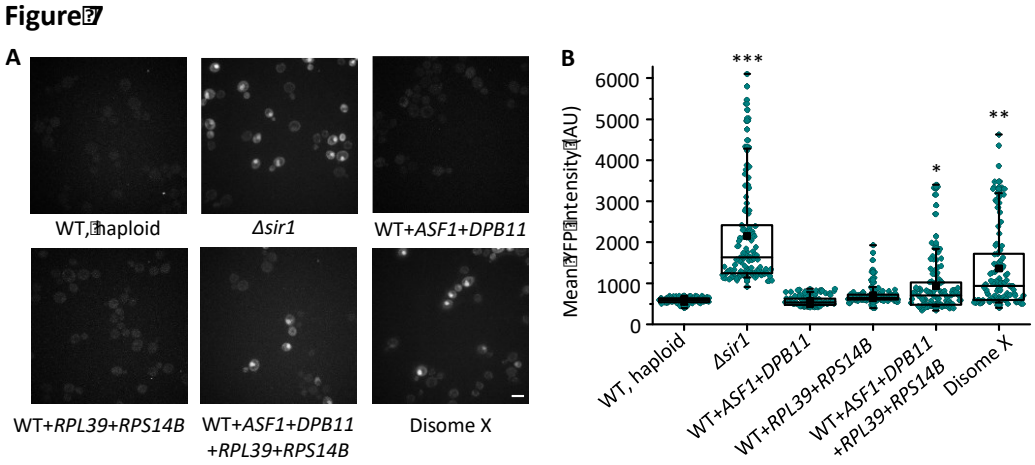
Figure 7
A
WT, haploid
Δsir1
WT+ASF1+DPB11
WT+RPL39+RPS14B
WT+ASF1+DPB11 +RPL39+RPS14B
Disome X
B
Mean YFP intensity (AU)
6000
5000
4000
3000
2000
1000
0
***
**
*
WT, haploid
Δsir1
WT+ASF1+DPB11
WT+RPL39+RPS14B
WT+ASF1+DPB11 +RPL39+RPS14B
Disome X

3.8 Supplementary Figures

3.8.1 Figure 1 – figure supplement 1:

Figure 1 - figure supplement 1

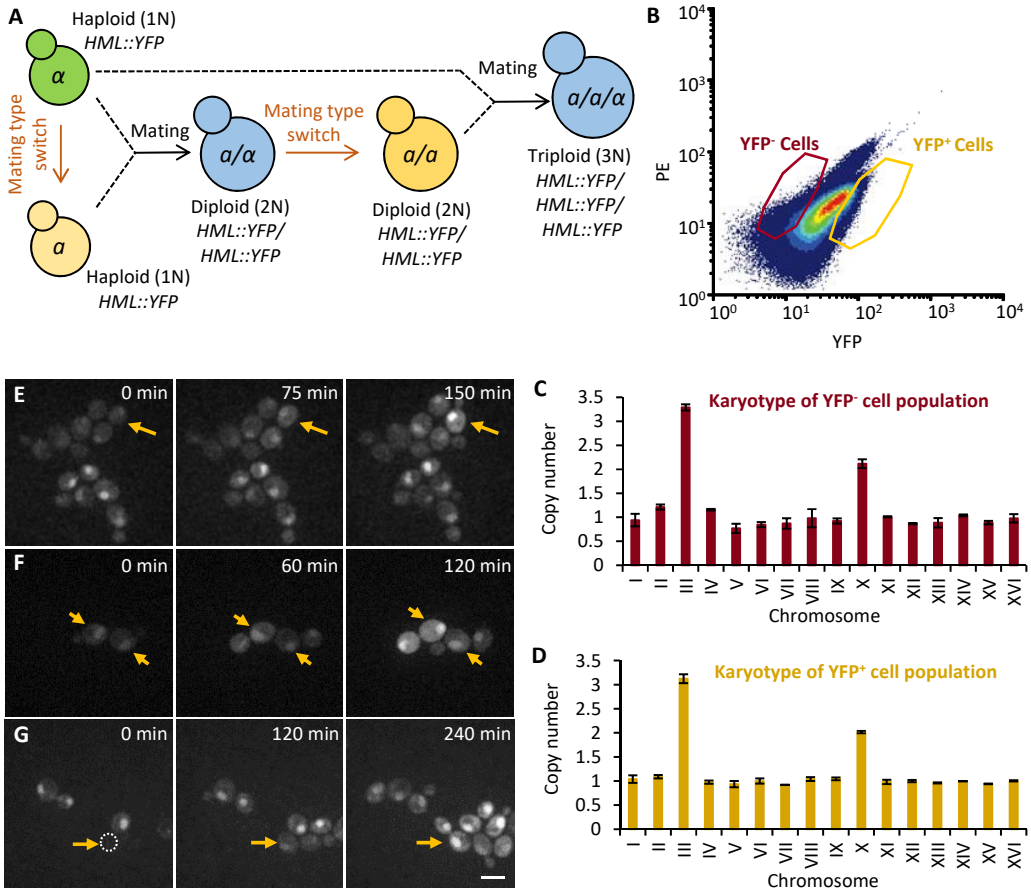

3.8.2 Figure 5 – figure supplement 1:

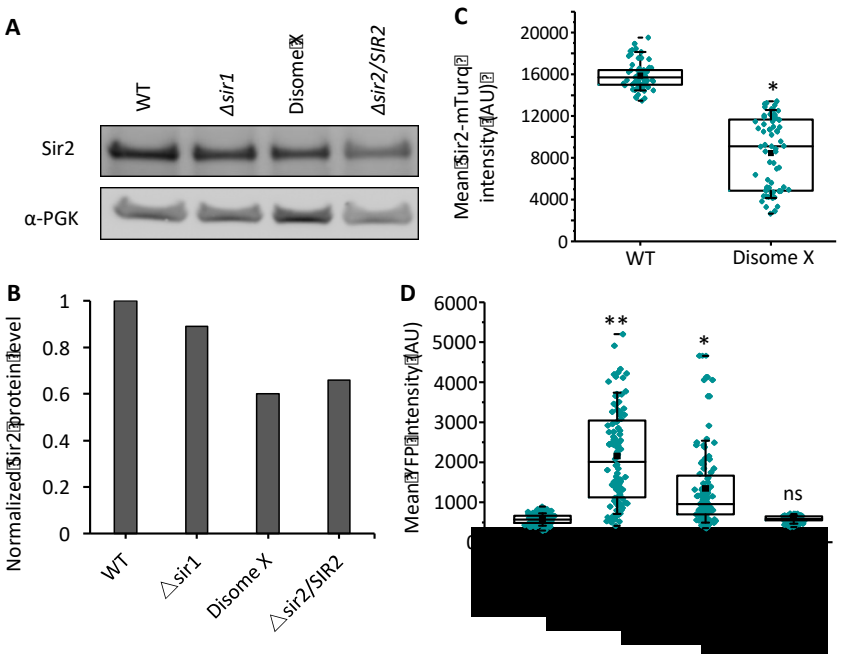

3.8.3 Figure 6 – figure supplement 1:

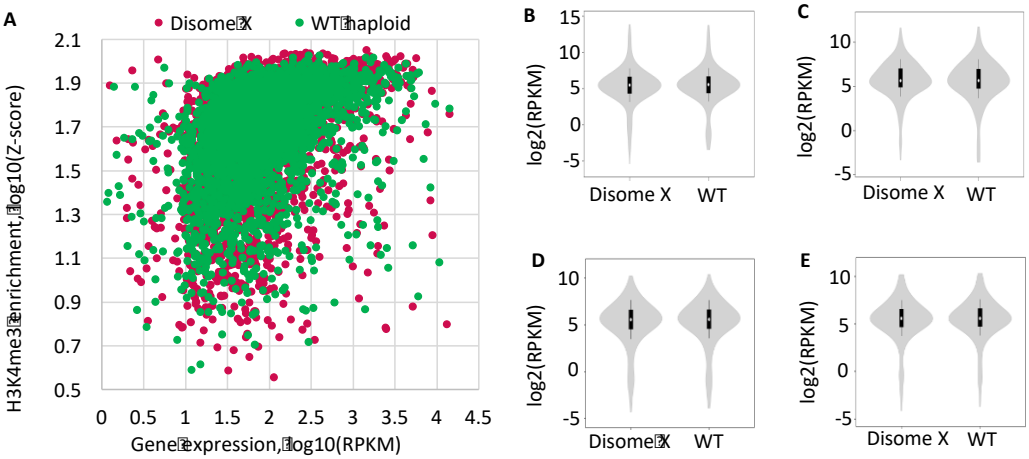

3.9 Tables

3.9.1 Table 1: List of stable aneuploid karyotypes exhibiting defective silencing of the *HML* locus.

Name	Basal Ploidy	I	II	III	IV	V	VI	VII	VIII	IX	X	XI	XII	XIII	XIV	XV	XVI
RLY9071	2N	1	2	2	2	1	2	1	1	2	2	1	2	2	2	2	2
RLY9072	2N	2	2	3	2	2	2	2	2	2	2	2	2	3	2	2	2
RLY9073	2N	3	2	2	2	2	2	2	2	2	3	2	3	2	2	2	2
RLY9074	2N	2	2	2	2	2	2	2	2	3	2	2	2	2	2	2	3
RLY9075	1N	1	2	1	1	1	1	1	1	1	1	1	1	2	1	1	1
RLY9076	1N	1	1	3	1	1	1	1	1	1	2	1	1	1	1	1	1
RLY9077	1N	2	1	1	1	1	1	1	1	1	2	1	2	2	1	1	1
RLY9078	1N	1	1	2	1	2	1	1	1	1	1	1	2	1	1	1	1
RLY9079	1N	1	1	1	1	1	1	1	2	2	2	1	1	2	2	1	1
RLY9080	1N	1	1	1	1	1	1	1	1	2	1	1	1	2	1	2	1
RLY9081	1N	1	1	1	1	1	1	1	1	1	2	1	2	2	1	1	1
RLY9082	1N	1	1	2	1	1	1	1	1	1	1	1	2	1	1	1	1
RLY9083	1N	1	1	2	1	1	1	1	1	2	1	1	1	2	1	1	1
RLY9084	1N	1	2	1	1	1	1	1	1	1	1	1	2	1	1	1	1
RLY9085	1N	1	1	2	1	1	1	1	1	1	2	1	1	1	1	1	2
RLY9086	1N	1	1	2	1	1	1	1	2	1	1	1	1	1	1	1	2
RLY9087	1N	1	1	1	1	1	1	1	1	2	1	1	1	1	1	2	2
RLY9088	1N	2	2	1	1	1	1	1	1	1	2	1	2	1	1	1	1
RLY9089	1N	1	2	1	1	1	1	1	1	1	1	1	1	2	1	1	2
RLY9090	1N	1	1	2	1	1	1	1	1	1	1	2	2	1	1	1	1
RLY9091	1N	1	1	1	1	1	1	1	2	1	2	1	1	1	1	1	1
RLY9092	1N	2	1	1	2	1	1	1	1	1	1	1	1	1	1	1	1
RLY9093	1N	1	1	1	1	1	1	1	1	1	2	1	1	1	1	1	2
RLY9094	1N	1	1	2	1	1	1	1	1	1	2	1	1	1	1	1	1

3.9.2 Table 2: The number of genes plotted for each category in Figure 6A-B and Figure 6 – figure supplement 1 is listed.

H3K4me3	**Category I**: Genome-wide	**Category II**: Differentially down-regulated genes in disome X	**Category III:** Differentially up-regulated genes in disome X	**Category IV:** Subtelomeric (out of 220 genes located in 15kb region at both ends of chromosomes)
Number of genes with H3K4me3 score present in both disome X and WT	3502	24	24	18
Number of genes with H3K4me3 score present in disome X but not in WT	197	0	11	6
Number of genes with H3K4me3 score present in WT but not in disome X	289	3	6	3
Number of genes without H3K4me3 score but expressed in both disome X and WT	2196	65	121	75
Total	6184	92	162	102
H3K79me3	**Category I**: Genome-wide	**Category II**: Differentially down-regulated genes in disome X	**Category III:** Differentially up-regulated genes in disome X	**Category IV:** Subtelomeric (out of 220 genes located in 15kb region at both ends of chromosomes)
Number of genes with H3K79me3 score present in both disome X and WT	2249	6	6	6
Number of genes with H3K79me3 score present in disome X but not in WT	364	2	2	4
Number of genes with H3K79me3 score present in WT but not in disome X	255	4	1	1
Number of genes without H3K79me3 score but expressed in both disome X and WT	3316	80	153	91
Total	6184	92	162	102

3.9.3 Table 3: List of top 15 candidates from gain-of-copy-number screen.

Genotype	Desilencing score relative to disome X	Description of gene
Disome X	1	--
WT+SRS2	0.568966	DNA helicase and DNA-dependent ATPase; involved in DNA repair and checkpoint recovery, affects genome stability; functional homolog of human RTEL1.
WT+DPB11	0.53	DNA replication initiation protein; loads DNA pol epsilon onto pre-replication complexes at origins; ortholog of human TopBP1.
WT+RPL39	0.489655	Ribosomal 60S subunit protein L39; required for ribosome biogenesis; loss of both Rpl31p and Rpl39p confers lethality; homologous to mammalian ribosomal protein L39.
WT+ASF1	0.489483	Nucleosome assembly factor; involved in chromatin assembly, disassembly.
WT+RPS14B	0.481724	Protein component of the small (40S) ribosomal subunit; required for ribosome assembly and 20S pre-rRNA processing; homologous to mammalian ribosomal protein S14 and bacterial S11.
WT+PRE3	0.422759	Beta 1 subunit of the 20S proteasome; responsible for cleavage after acidic residues in peptides.
WT+SPT10	0.387069	Histone H3 acetylase with a role in transcriptional regulation; involved in S phase-specific acetylation of H3K56 at histone promoters, which is required for recruitment of SWI/SNF nucleosome remodeling complex.
WT+CYR1	0.358621	Adenylate cyclase; the cAMP pathway controls a variety of cellular processes, including metabolism, cell cycle, stress response, stationary phase, and sporulation.
WT+HIR3	0.331552	Subunit of the HIR complex; a nucleosome assembly complex involved in regulation of histone gene transcription; involved in position-dependent gene silencing and nucleosome reassembly; ortholog of human CABIN1 protein.
WT+RTT101	0.31569	Cullin subunit of a Roc1p-dependent E3 ubiquitin ligase complex; role in anaphase progression; required for recovery after DSB repair.
WT+RPA34	0.295	RNA polymerase I subunit A34.5; essential for nucleolar assembly and for high polymerase loading rate; nucleolar localization depends on Rpa49p.
WT+SWI3	0.291552	Subunit of the SWI/SNF chromatin remodeling complex; SWI/SNF regulates transcription by remodeling chromosomes.
WT+MIR1	0.269138	Mitochondrial phosphate carrier; imports inorganic phosphate into mitochondria.
WT+VPS25	0.268103	Component of the ESCRT-II complex; ESCRT-II is involved in ubiquitin-dependent sorting of proteins into the endosome.
WT+NUP85	0.254483	Subunit of the Nup84p subcomplex of the nuclear pore complex (NPC); plays roles in several processes that may require localization of genes or chromosomes at the nuclear periphery, and chromatin silencing; homologous to human NUP85 aka NUP75.

3.9.4 Table 4: List of yeast strains used in this study, and not listed in **table 1.**

Name	Genotype	Experiment
RLY9017	*MATα; ura3; his3; trp1; leu2; hml::P_{URA3}-NLS-YFP*	Fig 1B, 1D, 1E, Fig 1-S1A; Fig 2A, 2B, 2D; Fig 5-S1A,B,D; Fig 6A-D; Fig 6-S1, Fig 6-Sup table 1
RLY9018	*MATa; ura3; his3; trp1; leu2; hml::P_{URA3}-NLS-YFP*	Fig 1-S1A
RLY9019	*MATa/α; RLY9017 × RLY9017*	Fig 1-S1A
RLY9020	*MATa/a; (derived from RLY9019 by mating type switching)*	Fig 1-S1A
RLY9021	*MATa/a/α; RLY9020 × RLY9017*	Fig 1-S1A
RLY9022	*RLY9017; sir1Δ::KanMX6*	Fig 1B, 1D; Fig 2A, 2D,
RLY9023*	*ura3; his3; trp1; leu2; hml::P_{URA3}-NLS-YFP/hml::P_{URA3}-NLS-YFP; + Chr III*	Fig 2A
RLY9024*	*ura3; his3; trp1; leu2; hml::P_{URA3}-NLS-YFP/hml::P_{URA3}-NLS-YFP/hml::P_{URA3}-NLS-YFP; + Chr III; + Chr III (haploid strain with two extra copies of Chr III)*	Fig 2A, 2B
RLY9025	*MATa; ura3; his3; trp1; leu2; hml::P_{URA3}-NLS-YFP; + Chr X (derived from RLY9076)*	Fig 2A, 2C, 2D, Fig 6A-D, Fig 6-S1A-E, Fig 6-Sup table 1
RLY9026	*MATa; ura3; his3; trp1; leu2; hml::P_{URA3}-NLS-YFP; + Chr X (derived from RLY9077)*	Fig 2A
RLY9027*	*ura3; his3; trp1; leu2; hml::P_{URA3}-NLS-YFP; + Chr I; + Chr XII; + Chr XIII (derived from RLY9077)*	Fig 2A
RLY9028	*RLY9017; Chr X::P_{gal1}-URA^{KL}-Chr X*	Fig 2C
RLY9029	*RLY9017; Chr X::P_{gal1}-URA^{KL}-CenX*	Fig 2C
RLY9030	*RLY9024; Chr X::P_{gal1}-URA^{KL}-Chr X*	Fig 2C
RLY9031	*RLY9024; Chr X::P_{gal1}-URA^{KL}-CenX*	Fig 2C
RLY9032	*RLY9025; sir1Δ::KanMX6;*	Fig 2D
RLY9033	*MATa; ura3; his3; trp1; leu2;*	Fig 3A-B
RLY9034	*MATa; ura3; his3; trp1; leu2; sir1Δ:: KanMX6*	Fig 3A-B
RLY9035	*MATa; ura3; his3; trp1; leu2; + Chr X*	Fig 3A-B
RLY9036	*RLY9017; SIR2::HA-HIS3*	Fig 4A-D
RLY9037	*RLY9022; SIR2::HA-HIS3*	Fig 4A-D
RLY9038	*RLY9026; SIR2::HA-HIS3*	Fig 4A-D
RLY9039	*RLY9017; SIR2::mTurq-KanMX6*	Fig 5A-B, Fig 5-S1C
RLY9040	*RLY9025; SIR2::mTurq-KanMX6; + Chr X*	Fig 5A-B, Fig 5-S1C
RLY9041	*RLY9033; hmlprox::lacO(256)-LEU2; HIS3::P_{URA3}-LacI::GFP-KanMX; NUP60::mCherry-URA3*	Fig 5C
RLY9042	*RLY9035; hmlprox::lacO(256)-LEU2; HIS3::P_{URA3}-LacI::GFP-KanMX; + Chr X; NUP60::mCherry-URA3; + Chr X*	Fig 5C

RLY9043	*RLY9017; + URA3 (Integration of NcoI digested pRS306, URA3)*	Fig 7A-B
RLY9044	*RLY9022; + URA3 (Integration of NcoI digested pRS306, URA3)*	Fig 7A-B
RLY9045	*RLY9025; + URA3 (Integration of NcoI digested pRS306, URA3)*	Fig 7A-B
RLY9046	*RLY9017; + ASF1 + DPB11 (Integration of NcoI digested pWM1 into URA3 locus)*	Fig 7A-B
RLY9047	*RLY9018; + RPL39 + RPS14B (Integration of HpaI digested pWM2 into DPB11 locus)*	Fig 7A-B
RLY9048*	*ura3; his3; trp1; leu2; hml::P_{URA3}-NLS-YFP; + RPL39 + RPS14B + ASF1 + DPB11*	Fig 7A-B
RLY9049	*RLY9025; + Chr X; + Moby plasmid without ORF, CEN-ARS, URA3*	Fig 7-Sup table 1
RLY9050	*RLY9017; + PRE3 (YJL001W, MOBY-ORF, CEN-ARS, URA3)*	Fig 7-Sup table 1
RLY9051	*RLY9017; + CYR1 (YJL005W, MOBY-ORF, CEN-ARS, URA3)*	Fig 7-Sup table 1
RLY9052	*RLY9017; + RTT101 (YJL047C, MOBY-ORF, CEN-ARS, URA3)*	Fig 7-Sup table 1
RLY9053	*RLY9017; + DPB11 (YJL090C, MOBY-ORF, CEN-ARS, URA3)*	Fig 7-Sup table 1
RLY9054	*RLY9017; + SRS2 (YJL092W, MOBY-ORF, CEN-ARS, URA3)*	Fig 7-Sup table 1
RLY9055	*RLY9017; + ASF1 (YJL115W, MOBY-ORF, CEN-ARS, URA3)*	Fig 7-Sup table 1
RLY9056	*RLY9017; + SPT10 (YJL127C, MOBY-ORF, CEN-ARS, URA3)*	Fig 7-Sup table 1
RLY9057	*RLY9017; + RPA34 (YJL148W, MOBY-ORF, CEN-ARS, URA3)*	Fig 7-Sup table 1
RLY9058	*RLY9017; + SWI3 (YJL176C, MOBY-ORF, CEN-ARS, URA3)*	Fig 7-Sup table 1
RLY9059	*RLY9017; + RPL39 (YJL189W, MOBY-ORF, CEN-ARS, URA3)*	Fig 7-Sup table 1
RLY9060	*RLY9017; + RPS14B (YJL191W, MOBY-ORF, CEN-ARS, URA3)*	Fig 7-Sup table 1
RLY9061	*RLY9017; + NUP85 (YJR042W, MOBY-ORF, CEN-ARS, URA3)*	Fig 7-Sup table 1
RLY9062	*RLY9017; + MIR1 (YJR077C, MOBY-ORF, CEN-ARS, URA3)*	Fig 7-Sup table 1
RLY9063	*RLY9017; + VPS25 (YJR102C, MOBY-ORF, CEN-ARS, URA3)*	Fig 7-Sup table 1
RLY9064	*RLY9017; + HIR3 (YJR140C, MOBY-ORF, CEN-ARS, URA3)*	Fig 7-Sup table 1
RLY9065	*RLY9019; sir2Δ::KanMX6/SIR2*	Fig 5-S1A,B,D

* matying type unknown

KL, Kluyveromyces lactis

3.9.5 Table 5: List of plasmids used in this study.

Name	RLB No.	Description	Source
pWM1	*RLB912*	*pRS306, RPL39, RPS14B*	This study
pWM2	*RLB913*	*pRS306, ASF1, DPB11*	This study
pWM3	*RLB884*	*KAN, URA3, CEN-ARS, (MOBY plasmid without ORF)*	Li Lab
pWM4	*RLB914*	*AMP, URA3, CEN-ARS, (pRS316-P_{gal1}-URA3)*	Li Lab

Chapter 4

Summary and Discussion

Some contents in this chapter are adapted from:

Aneuploidy as a cause of impaired chromatin silencing and mating-type specification in budding yeast. Mulla WA, Seidel CW, Zhu J, Tsai HJ, Smith SE, Singh P, Bradford WD, McCroskey S, Nelliat AR, Conkright J, Peak A, Malanowski KE, Perera AG, Li R. eLife 2017.

4.1 Loss of chromatin silencing is associated with specific karyotypic features

Our unbiased approach to identify chromosome stoichiometries associated with disrupted chromatin silencing revealed that Chr III and Chr X were frequently gained in cells lacking stable silencing at the *HML* locus. Notably, this pattern of chromosome enrichment was significantly different from that found in viable, karyotypically-stable aneuploid strains obtained through triploid meiosis (Pavelka, Rancati et al. 2010), suggesting that chromatin desilencing is not an obligatory outcome of abnormal chromosome numbers, but rather, is caused by specific chromosome imbalance. We expected that Chr III and Chr XII would be enriched in our screen since extra copies of these chromosomes would increase the copy number of heterochromatic DNA, which could potentially titrate silencing factors (Smith, Brachmann et al. 1998, Michel, Kornmann et al. 2005, Dodson and Rine 2015). However, only chromosome III gain was enriched and contributes to desilencing, but it was insufficient on its own for significant desilencing. Chr X, by contrast, lacks any known regions of silenced chromatin other than the subtelomeric DNA, and so the effect of extra copies of this chromosome was unlikely to be related to the titration of silencing factors. Our functional analysis suggests that the mechanisms underlying disome X-associated desilencing are complex (discussed further below).

It is important to point out that the aneuploid karyotypes that we identified did not appear to lead to a single state of chromatin silencing or desilencing but instead resulted in heterogeneous populations of cells with respect to gene expression from the normally silenced chromatin regions. Although the different levels of YFP expression in individual YFP^+ cells might be due to the natural gene expression noise, the co-existence of

considerable fractions of both YFP^+ and YFP^- cells in each of the aneuploid populations suggests that these karyotypes lead to instability of the epigenetic state that is stably inherited in normal haploid cells.

4.2 The impact of Chr X disomy on histone modifications at silenced and non-silenced loci

H3K4 trimethylation is considered to be a mark of active transcription, given that its occupancy is generally high at the promoters of actively transcribed genes (Pokholok, Harbison et al. 2005, Guillemette, Drogaris et al. 2011). Supporting this notion, our studies show a positive correlation between enrichment of this histone mark and transcriptional activity in both haploid and aneuploid strains. In yeast, H3K4 trimethylation is carried out by the Set1 complex and transcriptional outcomes related to changes in this mark are partially dependent on the location of genes in active or silent chromatin regions (Bryk, Briggs et al. 2002, Krogan, Dover et al. 2002, Santos-Rosa, Schneider et al. 2002). Although H3K4 is generally hypermethylated within regions of euchromatin and hypomethylated within heterochromatin, loss of H3K4me3 due to deletion of *SET1* had little effect on coding gene expression (Margaritis, Oreal et al. 2012). Consistently, our transcriptome analysis in disome X strains does not show a correlation between H3K4me3 and global transcriptional activation. However, in the case of silent domains, such as subtelomeric genes, we indeed found that both H3K4me3 modifications and gene expression were increased in disome X cells compared with the haploid control strain. The significant changes in histone modification patterns, combined with transcriptional derepression at many loci in regions of silent chromatin (mating-type loci, *rDNA,* and

subtelomeric DNA) in disome X demonstrated that aneuploidy has the capacity to alter the histone-modification profile. It should be noted, however, that RNA-seq data showed that most of the subtelomeric genes are not strongly affected by Chr X disomy, suggesting that this aneuploidy does not have a general effect on silencing at subtelomeres. However, this is consistent with the previous observation that expression of subtelomeric genes in *S. cerevisiae* is largely uninfluenced by mutations in Sir proteins and Sir-based silencing is not a widespread phenomenon at telomeres despite strong enrichment of Sir proteins at telomeric regions (Takahashi, Schulze et al. 2011, Ellahi, Thurtle et al. 2015)**.**

4.3 Potential mechanisms by which Chr X disomy disrupts stable epigenetic inheritance

We investigated several non-mutually exclusive mechanisms by which gain of Chr X could disrupt stable chromatin silencing. First, the defect in silencing could be due to a moderately reduced Sir2 level in Disome X compared to haploid (Figure 5 - figure supplement 1A-C). However, this is unlikely because previous study (Dodson and Rine 2015) and our own experiments showed that *SIR2* is not haploinsufficient for silencing: heterozygous *SIR2* diploid strain (*Δsir2/SIR2*), in which Sir2 level was reduced by an extent similar to that in disome X, did not compromise *HML* silencing (Figure 5 - figure supplement 1D). Second, we explored the possibility that NAD biosynthesis could be compromised because three genes (*BNA1, BNA2, BNA4*) involved in this pathway are located on Chr X, and low NAD levels have been linked to defective silencing phenotypes (Grozinger, Chao et al. 2001, Sandmeier, Celic et al. 2002, Bedalov, Hirao et al. 2003). However, supplementing disome X strains with NAD did not rescue the desilencing

phenotype (data not shown). Third, our comprehensive screen for Chr X genes showed that a combination of four genes partially recapitulated the desilencing phenotype of disome X when each is increased by only a single copy. The known functions of these four genes are diverse, ranging from ribosomal components to a histone chaperone and a DNA polymerase subunit, suggesting that chromatin desilencing in disome X results from the combinatorial effects of multiple pathways that may each contribute to the establishment of the silenced chromatin. This is consistent with previous studies showing that aneuploidy confers complex or significant phenotypic changes by multigenic mechanisms (Selmecki, Forche et al. 2006, Rancati, Pavelka et al. 2008, Selmecki, Gerami-Nejad et al. 2008, Pavelka, Rancati et al. 2010, Chen, Bradford et al. 2012, Chen, Mulla et al. 2015).

Another possible mechanism by which aneuploidy could impact silencing is by affecting the defined chromosome organization within the nucleus, whereby heterochromatin-like regions are tethered to the nuclear periphery and form a specialized structural compartment, which is required for Sir proteins to establish silencing (Andrulis, Neiman et al. 1998, Mekhail, Seebacher et al. 2008, Bystricky, Van Attikum et al. 2009, Ruault, De Meyer et al. 2011). Indeed, our results show reduced attachment of the *HML* locus to the nuclear envelope in disome X cells. The diffused Sir2 distribution, particularly in cells with desilenced *HML* gene expression, is consistent with previous reports that the silencing function of this protein requires its concentration to perinuclear pools (Hoppe, Tanny et al. 2002, Taddei, Van Houwe et al. 2009). However, it is presently unclear whether the insufficient tethering of chromosome regions to be silenced to the nuclear periphery or failed concentration of Sir2 to this area of the nucleus is directly caused by the increased copy number of the relevant genes on Chr X. Studies of the transcriptome in

trisomy 21 human fibroblasts show that, although the overall nuclear organization defined by lamin-associated domains (LADs) is intact in these cells, alterations in H3K4me3 correlate with specialized gene expression dysregulation domains (GEDDs) (Letourneau, Santoni et al. 2014). This finding together with our results suggests that a perturbed nuclear compartmentalization, which causes changes in gene expression, may be an emergent outcome of gene copy number imbalance associated with certain chromosome aneuploidy. However, our data do not clarify whether the altered chromatin positioning or *HML* perinuclear localization in disome X strain was a cause or consequence of chromatin desilencing.

Epigenetic states are acquired through a precise balance between euchromatin and heterochromatin and are an essential mechanism to control proper cellular identity (Jaenisch and Bird 2003). Here, we have shown that numerical alterations in chromosomes can derepress heterochromatin to break this delicate balance, relax epigenetic inheritance, and cause stochastic variation in cell identity that impairs the responsiveness to regulatory factors. Our findings provide the causal evidence that aneuploidy is a source of epigenetic instability. It may thus be worth exploring a potential linkage between epigenetic dysregulation and chromosome copy number alterations observed in cancer. The aneuploidy-induced changes in heterochromatin inheritance and histone-modification landscape may be an important mechanism by which chromosomal instability drives large-scale phenotypic variability during tumor evolution.

References:

Aguilera, A. and B. Gomez-Gonzalez (2008). "Genome instability: a mechanistic view of its causes and consequences." Nat Rev Genet **9**(3): 204-217.

Anders, K., J. Kudrna, K. Keller, B. Kinghorn, E. Miller, D. Pauw, A. Peck, C. Shellooe and I. Strong (2009). "A strategy for constructing aneuploid yeast strains by transient nondisjunction of a target chromosome." BMC Genetics **10**(1): 36.

Anders, K. R., J. R. Kudrna, K. E. Keller, B. Kinghorn, E. M. Miller, D. Pauw, A. T. Peck, C. E. Shellooe and I. J. Strong (2009). "A strategy for constructing aneuploid yeast strains by transient nondisjunction of a target chromosome." BMC Genet **10**: 36.

Andrulis, E. D., A. M. Neiman, D. C. Zappulla and R. Sternglanz (1998). "Perinuclear localization of chromatin facilitates transcriptional silencing." Nature **394**(6693): 592-595.

Arbour, M., E. Epp, H. Hogues, A. Sellam, C. Lacroix, J. Rauceo, A. Mitchell, M. Whiteway and A. Nantel (2009). "Widespread occurrence of chromosomal aneuploidy following the routine production of Candida albicans mutants." FEMS Yeast Res **9**(7): 1070-1077.

Bedalov, A., M. Hirao, J. Posakony, M. Nelson and J. A. Simon (2003). "NAD+-dependent deacetylase Hst1p controls biosynthesis a cellular NAD+ levels in Saccharomyces cerevisiae." Mol Cell Biol **23**(19): 7044-7054.

Behrouzi, R., C. Lu, M. A. Currie, G. Jih, N. Iglesias and D. Moazed (2016). "Heterochromatin assembly by interrupted Sir3 bridges across neighboring nucleosomes." Elife **5**.

Belyi, V. A., P. Ak, E. Markert, H. Wang, W. Hu, A. Puzio-Kuter and A. J. Levine (2010). "The origins and evolution of the p53 family of genes." Cold Spring Harb Perspect Biol **2**(6): a001198.

Bennett, R. J. and A. D. Johnson (2003). "Completion of a parasexual cycle in Candida albicans by induced chromosome loss in tetraploid strains." EMBO J **22**(10): 2505-2515.

Birchler, J. A. (2010). "Reflections on studies of gene expression in aneuploids." Biochem J **426**(2): 119-123.

Botstein, D. and G. R. Fink (2011). "Yeast: an experimental organism for 21st Century biology." Genetics **189**(3): 695-704.

Bouchonville, K., A. Forche, K. E. Tang, A. Selmecki and J. Berman (2009). "Aneuploid chromosomes are highly unstable during DNA transformation of Candida albicans." Eukaryot Cell **8**(10): 1554-1566.

Boveri, T. (1914). "Zur Frage der Entstehung maligner Tumoren." Jena, Gustav Fisher Verlag, Germany.

Bryk, M., S. D. Briggs, B. D. Strahl, M. J. Curcio, C. D. Allis and F. Winston (2002). "Evidence that Set1, a factor required for methylation of histone H3, regulates rDNA silencing in S. cerevisiae by a Sir2-independent mechanism." Curr Biol **12**(2): 165-170.

Buhler, M. and S. M. Gasser (2009). "Silent chromatin at the middle and ends: lessons from yeasts." EMBO J **28**(15): 2149-2161.

Bystricky, K., H. Van Attikum, M. D. Montiel, V. Dion, L. Gehlen and S. M. Gasser (2009). "Regulation of nuclear positioning and dynamics of the silent mating type loci by the yeast Ku70/Ku80 complex." Mol Cell Biol **29**(3): 835-848.

Campbell, D., J. S. Doctor, J. H. Feuersanger and M. M. Doolittle (1981). "Differential mitotic stability of yeast disomes derived from triploid meiosis." Genetics **98**(2): 239-255.

Charles, J. S., M. L. Hamilton and T. D. Petes (2010). "Meiotic Chromosome Segregation in Triploid Strains of Saccharomyces cerevisiae." Genetics **186**(2): 537-550.

Chen, G., W. D. Bradford, C. W. Seidel and R. Li (2012). "Hsp90 stress potentiates rapid cellular adaptation through induction of aneuploidy." Nature **482**(7384): 246-250.

Chen, G., W. A. Mulla, A. Kucharavy, H. J. Tsai, B. Rubinstein, J. Conkright, S. McCroskey, W. D. Bradford, L. Weems, J. S. Haug, C. W. Seidel, J. Berman and R. Li (2015). "Targeting the adaptability of heterogeneous aneuploids." Cell **160**(4): 771-784.

Chen, X., B. B. Magee, D. Dawson, P. T. Magee and C. A. Kumamoto (2004). "Chromosome 1 trisomy compromises the virulence of Candida albicans." Mol Microbiol **51**(2): 551-565.

Conde, J. and G. R. Fink (1976). "A mutant of Saccharomyces cerevisiae defective for nuclear fusion." Proceedings of the National Academy of Sciences **73**(10): 3651-3655.

Darzynkiewicz, Z., H. D. Halicka and H. Zhao (2010). "Analysis of cellular DNA content by flow and laser scanning cytometry." Adv Exp Med Biol **676**: 137-147.

Didelot, X., R. Bowden, D. J. Wilson, T. E. Peto and D. W. Crook (2012). "Transforming clinical microbiology with bacterial genome sequencing." Nat Rev Genet **13**(9): 601-612.

Dion, B. and G. W. Brown (2009). "Comparative genome hybridization on tiling microarrays to detect aneuploidies in yeast." Methods Mol Biol **548**: 1-18.

Dodson, A. E. and J. Rine (2015). "Heritable capture of heterochromatin dynamics in Saccharomyces cerevisiae." Elife **4**: e05007.

Doi, M., M. Homma, A. Chindamporn and K. Tanaka (1992). "Estimation of chromosome number and size by pulsed-field gel electrophoresis (PFGE) in medically important Candida species." J Gen Microbiol **138**(10): 2243-2251.

Dudarewicz, L., W. Holzgreve, A. Jeziorowska, L. Jakubowski and B. Zimmermann (2005). "Molecular methods for rapid detection of aneuploidy." J Appl Genet **46**(2): 207-215.

Duncan, A. W. (2013). "Aneuploidy, polyploidy and ploidy reversal in the liver." Semin Cell Dev Biol **24**(4): 347-356.

Ellahi, A., D. M. Thurtle and J. Rine (2015). "The Chromatin and Transcriptional Landscape of Native Saccharomyces cerevisiae Telomeres and Subtelomeric Domains." Genetics **200**(2): 505-521.

Feinberg, A. P., R. Ohlsson and S. Henikoff (2006). "The epigenetic progenitor origin of human cancer." Nat Rev Genet **7**(1): 21-33.

Forche, A., D. Abbey, T. Pisithkul, M. A. Weinzierl, T. Ringstrom, D. Bruck, K. Petersen and J. Berman (2011). "Stress Alters Rates and Types of Loss of Heterozygosity in Candida albicans." mBio **2**(4).

Gresham, D., M. M. Desai, C. M. Tucker, H. T. Jenq, D. A. Pai, A. Ward, C. G. DeSevo, D. Botstein and M. J. Dunham (2008). "The repertoire and dynamics of evolutionary adaptations to controlled nutrient-limited environments in yeast." PLoS Genet **4**(12): e1000303.

Grozinger, C. M., E. D. Chao, H. E. Blackwell, D. Moazed and S. L. Schreiber (2001). "Identification of a class of small molecule inhibitors of the sirtuin family of NAD-dependent deacetylases by phenotypic screening." J Biol Chem **276**(42): 38837-38843.

Guillemette, B., P. Drogaris, H. H. Lin, H. Armstrong, K. Hiragami-Hamada, A. Imhof, E. Bonneil, P. Thibault, A. Verreault and R. J. Festenstein (2011). "H3 lysine 4 is acetylated at active gene promoters and is regulated by H3 lysine 4 methylation." PLoS Genet **7**(3): e1001354.

Haase, S. B. and D. J. Lew (1997). "Flow cytometric analysis of DNA content in budding yeast." Methods Enzymol **283**: 322-332.

Hartwell, L. H. and D. Smith (1985). "Altered fidelity of mitotic chromosome transmission in cell cycle mutants of S. cerevisiae." Genetics **110**(3): 381-395.

Hill, A. and K. Bloom (1987). "Genetic manipulation of centromere function." Molecular and Cellular Biology **7**(7): 2397-2405.

Ho, C. H., L. Magtanong, S. L. Barker, D. Gresham, S. Nishimura, P. Natarajan, J. L. Koh, J. Porter, C. A. Gray, R. J. Andersen, G. Giaever, C. Nislow, B. Andrews, D. Botstein, T. R. Graham, M. Yoshida and C. Boone (2009). "A molecular barcoded yeast ORF library enables mode-of-action analysis of bioactive compounds." Nat Biotechnol **27**(4): 369-377.

Holland, A. J. and D. W. Cleveland (2009). "Boveri revisited: chromosomal instability, aneuploidy and tumorigenesis." Nat Rev Mol Cell Biol **10**(7): 478-487.

Holland, A. J. and D. W. Cleveland (2012). "Losing balance: the origin and impact of aneuploidy in cancer." EMBO Rep **13**(6): 501-514.

Hoppe, G. J., J. C. Tanny, A. D. Rudner, S. A. Gerber, S. Danaie, S. P. Gygi and D. Moazed (2002). "Steps in assembly of silent chromatin in yeast: Sir3-independent binding of a Sir2/Sir4 complex to silencers and role for Sir2-dependent deacetylation." Mol Cell Biol **22**(12): 4167-4180.

Hu, G., J. Wang, J. Choi, W. H. Jung, I. Liu, A. P. Litvintseva, T. Bicanic, R. Aurora, T. G. Mitchell, J. R. Perfect and J. W. Kronstad (2011). "Variation in chromosome copy number influences the virulence of Cryptococcus neoformans and occurs in isolates from AIDS patients." BMC Genomics **12**: 526.

Hughes, T. R., C. J. Roberts, H. Dai, A. R. Jones, M. R. Meyer, D. Slade, J. Burchard, S. Dow, T. R. Ward, M. J. Kidd, S. H. Friend and M. J. Marton (2000). "Widespread aneuploidy revealed by DNA microarray expression profiling." Nat Genet **25**(3): 333-337.

Hvorecny, K. L. and G. Prelich (2010). "A systematic CEN library of the Saccharomyces cerevisiae genome." Yeast **27**(10): 861-865.

Ibrahim, A. S., B. B. Magee, D. C. Sheppard, M. Yang, S. Kauffman, J. Becker, J. E. Edwards, Jr. and P. T. Magee (2005). "Effects of ploidy and mating type on virulence of Candida albicans." Infect Immun **73**(11): 7366-7374.

Jaenisch, R. and A. Bird (2003). "Epigenetic regulation of gene expression: how the genome integrates intrinsic and environmental signals." Nat Genet **33 Suppl**: 245-254.

Kanellis, P., M. Gagliardi, J. P. Banath, R. K. Szilard, S. Nakada, S. Galicia, F. D. Sweeney, D. C. Cabelof, P. L. Olive and D. Durocher (2007). "A Screen for Suppressors of Gross Chromosomal Rearrangements Identifies a Conserved Role for PLP in Preventing DNA Lesions." PLoS Genet **3**(8): e134.

Katan-Khaykovich, Y. and K. Struhl (2005). "Heterochromatin formation involves changes in histone modifications over multiple cell generations." EMBO J **24**(12): 2138-2149.

Klein, H. L. (2001). "Spontaneous Chromosome Loss in Saccharomyces cerevisiae Is Suppressed by DNA Damage Checkpoint Functions." Genetics **159**(4): 1501-1509.

Krogan, N. J., J. Dover, S. Khorrami, J. F. Greenblatt, J. Schneider, M. Johnston and A. Shilatifard (2002). "COMPASS, a histone H3 (Lysine 4) methyltransferase required for telomeric silencing of gene expression." J Biol Chem **277**(13): 10753-10755.

Kueng, S., M. Oppikofer and S. M. Gasser (2013). "SIR proteins and the assembly of silent chromatin in budding yeast." Annu Rev Genet **47**: 275-306.

Letourneau, A., F. A. Santoni, X. Bonilla, M. R. Sailani, D. Gonzalez, J. Kind, C. Chevalier, R. Thurman, R. S. Sandstrom, Y. Hibaoui, M. Garieri, K. Popadin, E. Falconnet, M. Gagnebin, C. Gehrig, A. Vannier, M. Guipponi, L. Farinelli, D. Robyr, E. Migliavacca, C. Borel, S. Deutsch, A. Feki, J. A. Stamatoyannopoulos, Y. Herault, B. van Steensel, R. Guigo and S. E. Antonarakis (2014). "Domains of genome-wide gene expression dysregulation in Down's syndrome." Nature **508**(7496): 345-350.

Li, C., J. E. Mueller and M. Bryk (2006). "Sir2 represses endogenous polymerase II transcription units in the ribosomal DNA nontranscribed spacer." Mol Biol Cell **17**(9): 3848-3859.

Liou, G. G., J. C. Tanny, R. G. Kruger, T. Walz and D. Moazed (2005). "Assembly of the SIR complex and its regulation by O-acetyl-ADP-ribose, a product of NAD-dependent histone deacetylation." Cell **121**(4): 515-527.

Mack, M., P. Gompel-Klein, E. Haase, J. Hietkamp, A. Ruhland and M. Brendel (1988). "Genetic characterization of hyperresistance to formaldehyde and 4-nitroquinoline-N-oxide in the yeast Saccharomyces cerevisiae." Mol Gen Genet **211**(2): 260-265.

Margaritis, T., V. Oreal, N. Brabers, L. Maestroni, A. Vitaliano-Prunier, J. J. Benschop, S. van Hooff, D. van Leenen, C. Dargemont, V. Geli and F. C. Holstege (2012). "Two distinct repressive mechanisms for histone 3 lysine 4 methylation through promoting 3'-end antisense transcription." PLoS Genet **8**(9): e1002952.

Maringele, L. and D. Lydall (2006). "Pulsed-field gel electrophoresis of budding yeast chromosomes." Methods Mol Biol **313**: 65-73.

Mayer, V. W. and A. Aguilera (1990). "High levels of chromosome instability in polyploids of Saccharomyces cerevisiae." Mutation Research/Fundamental and Molecular Mechanisms of Mutagenesis **231**(2): 177-186.

McGranahan, N., R. A. Burrell, D. Endesfelder, M. R. Novelli and C. Swanton (2012). "Cancer chromosomal instability: therapeutic and diagnostic challenges." EMBO Rep **13**(6): 528-538.

Mekhail, K. and D. Moazed (2010). "The nuclear envelope in genome organization, expression and stability." Nat Rev Mol Cell Biol **11**(5): 317-328.

Mekhail, K., J. Seebacher, S. P. Gygi and D. Moazed (2008). "Role for perinuclear chromosome tethering in maintenance of genome stability." Nature **456**(7222): 667-670.

Merlo, L. M., J. W. Pepper, B. J. Reid and C. C. Maley (2006). "Cancer as an evolutionary and ecological process." Nat Rev Cancer **6**(12): 924-935.

Michel, A. H., B. Kornmann, K. Dubrana and D. Shore (2005). "Spontaneous rDNA copy number variation modulates Sir2 levels and epigenetic gene silencing." Genes Dev **19**(10): 1199-1210.

Millar, C. B. and M. Grunstein (2006). "Genome-wide patterns of histone modifications in yeast." Nat Rev Mol Cell Biol **7**(9): 657-666.

Mitelman, F., B. Johansson and F. E. Mertens (2012). "Mitelman Database of Chromosome Aberrations and Gene Fusions in Cancer."

Morgan, M. A. and A. Shilatifard (2015). "Chromatin signatures of cancer." Genes Dev **29**(3): 238-249.

Morrow, C. A. and J. A. Fraser (2013). "Ploidy variation as an adaptive mechanism in human pathogenic fungi." Semin Cell Dev Biol.

Mulla, W., J. Zhu and R. Li (2014). "Yeast: a simple model system to study complex phenomena of aneuploidy." FEMS Microbiol Rev **38**(2): 201-212.

Musacchio, A. and E. D. Salmon (2007). "The spindle-assembly checkpoint in space and time." Nat Rev Mol Cell Biol **8**(5): 379-393.

Nagaoka, S. I., T. J. Hassold and P. A. Hunt (2012). "Human aneuploidy: mechanisms and new insights into an age-old problem." Nat Rev Genet **13**(7): 493-504.

Navin, N., J. Kendall, J. Troge, P. Andrews, L. Rodgers, J. McIndoo, K. Cook, A. Stepansky, D. Levy, D. Esposito, L. Muthuswamy, A. Krasnitz, W. R. McCombie, J. Hicks and M. Wigler (2011). "Tumour evolution inferred by single-cell sequencing." Nature **472**(7341): 90-94.

Nekrutenko, A. and J. Taylor (2012). "Next-generation sequencing data interpretation: enhancing reproducibility and accessibility." Nat Rev Genet **13**(9): 667-672.

Nilsson-Tillgren, T., J. L. Petersen, S. Holmberg and M. Kielland-Brandt (1980). "Transfer of chromosome III during *kar* mediated cytoduction in yeast." Carlsberg Research Communications **45**(2): 113-117.

Niwa, O., Y. Tange and A. Kurabayashi (2006). "Growth arrest and chromosome instability in aneuploid yeast." Yeast **23**(13): 937-950.

Niwa, O., Y. Tange and A. Kurabayashi (2006). "Growth arrest and chromosome instability in aneuploid yeast." Yeast **23**(13): 937-950.

Niwa, O. and M. Yanagida (1985). "Triploid meiosis and aneuploidy in Schizosaccharomyces pombe: an unstable aneuploid disomic for chromosome III." Current Genetics **9**(6): 463-470.

Nowell, P. C. (1976). "The clonal evolution of tumor cell populations." Science **194**(4260): 23-28.

O'Brien, F. G., E. E. Udo and W. B. Grubb (2006). "Contour-clamped homogeneous electric field electrophoresis of Staphylococcus aureus." Nat Protoc **1**(6): 3028-3033.

Osborne, E. A., S. Dudoit and J. Rine (2009). "The establishment of gene silencing at single-cell resolution." Nat Genet **41**(7): 800-806.

Ouspenski, I. I., S. J. Elledge and B. R. Brinkley (1999). "New yeast genes important for chromosome integrity and segregation identified by dosage effects on genome stability." Nucleic Acids Research **27**(15): 3001-3008.

Page, B. D. and M. Snyder (1993). "Chromosome Segregation in Yeast." Annual Review of Microbiology **47**(1): 231-261.

Pardo, B. and A. Aguilera (2012). "Complex chromosomal rearrangements mediated by break-induced replication involve structure-selective endonucleases." PLoS Genet **8**(9): e1002979.

Parry, E. M. and B. S. Cox (1970). "The tolerance of aneuploidy in yeast." Genetics Research **16**(03): 333-340.

Pavelka, N., G. Rancati and R. Li (2010). "Dr Jekyll and Mr Hyde: role of aneuploidy in cellular adaptation and cancer." Curr Opin Cell Biol **22**(6): 809-815.

Pavelka, N., G. Rancati, J. Zhu, W. D. Bradford, A. Saraf, L. Florens, B. W. Sanderson, G. L. Hattem and R. Li (2010). "Aneuploidy confers quantitative proteome changes and phenotypic variation in budding yeast." Nature **468**(7321): 321-325.

Pfau, S. J. and A. Amon (2012). "Chromosomal instability and aneuploidy in cancer: from yeast to man." EMBO Rep **13**(6): 515-527.

Pinkel, D. and D. G. Albertson (2005). "Array comparative genomic hybridization and its applications in cancer." Nat Genet **37 Suppl**: S11-17.

Pokholok, D. K., C. T. Harbison, S. Levine, M. Cole, N. M. Hannett, T. I. Lee, G. W. Bell, K. Walker, P. A. Rolfe, E. Herbolsheimer, J. Zeitlinger, F. Lewitter, D. K. Gifford and R. A. Young (2005). "Genome-wide map of nucleosome acetylation and methylation in yeast." Cell **122**(4): 517-527.

Polakova, S., C. Blume, J. A. Zarate, M. Mentel, D. Jorck-Ramberg, J. Stenderup and J. Piskur (2009). "Formation of new chromosomes as a virulence mechanism in yeast Candida glabrata." Proc Natl Acad Sci U S A **106**(8): 2688-2693.

Potapova, T., J. Zhu and R. Li (2013). "Aneuploidy and chromosomal instability: a vicious cycle driving cellular evolution and cancer genome chaos." Cancer and Metastasis Reviews: 1-13.

Rancati, G., N. Pavelka, B. Fleharty, A. Noll, R. Trimble, K. Walton, A. Perera, K. Staehling-Hampton, C. W. Seidel and R. Li (2008). "Aneuploidy underlies rapid adaptive evolution of yeast cells deprived of a conserved cytokinesis motor." Cell **135**(5): 879-893.

Rehen, S. K., Y. C. Yung, M. P. McCreight, D. Kaushal, A. H. Yang, B. S. Almeida, M. A. Kingsbury, K. M. Cabral, M. J. McConnell, B. Anliker, M. Fontanoz and J. Chun (2005). "Constitutional aneuploidy in the normal human brain." J Neurosci **25**(9): 2176-2180.

Reid, R. J., I. Sunjevaric, W. P. Voth, S. Ciccone, W. Du, A. E. Olsen, D. J. Stillman and R. Rothstein (2008). "Chromosome-scale genetic mapping using a set of 16 conditionally stable Saccharomyces cerevisiae chromosomes." Genetics **180**(4): 1799-1808.

Reid, R. J. D., I. Sunjevaric, W. P. Voth, S. Ciccone, W. Du, A. E. Olsen, D. J. Stillman and R. Rothstein (2008). "Chromosome-Scale Genetic Mapping Using a Set of 16 Conditionally Stable Saccharomyces cerevisiae Chromosomes." Genetics **180**(4): 1799-1808.

Reis, C. C., S. Batista and M. G. Ferreira (2012). "The fission yeast MRN complex tethers dysfunctional telomeres for NHEJ repair." EMBO J **31**(24): 4576-4586.

Ried, T., Y. Hu, M. J. Difilippantonio, B. M. Ghadimi, M. Grade and J. Camps (2012). "The consequences of chromosomal aneuploidy on the transcriptome of cancer cells." Biochim Biophys Acta **1819**(7): 784-793.

Ruault, M., A. De Meyer, I. Loiodice and A. Taddei (2011). "Clustering heterochromatin: Sir3 promotes telomere clustering independently of silencing in yeast." J Cell Biol **192**(3): 417-431.

Rusche, L. N., A. L. Kirchmaier and J. Rine (2003). "The establishment, inheritance, and function of silenced chromatin in Saccharomyces cerevisiae." Annu Rev Biochem **72**: 481-516.

Sandmeier, J. J., I. Celic, J. D. Boeke and J. S. Smith (2002). "Telomeric and rDNA silencing in Saccharomyces cerevisiae are dependent on a nuclear NAD(+) salvage pathway." Genetics **160**(3): 877-889.

Santos-Rosa, H., R. Schneider, A. J. Bannister, J. Sherriff, B. E. Bernstein, N. C. Emre, S. L. Schreiber, J. Mellor and T. Kouzarides (2002). "Active genes are tri-methylated at K4 of histone H3." Nature **419**(6905): 407-411.

Selmecki, A., A. Forche and J. Berman (2006). "Aneuploidy and isochromosome formation in drug-resistant Candida albicans." Science **313**(5785): 367-370.

Selmecki, A., M. Gerami-Nejad, C. Paulson, A. Forche and J. Berman (2008). "An isochromosome confers drug resistance in vivo by amplification of two genes, ERG11 and TAC1." Mol Microbiol **68**(3): 624-641.

Selmecki, A. M., K. Dulmage, L. E. Cowen, J. B. Anderson and J. Berman (2009). "Acquisition of aneuploidy provides increased fitness during the evolution of antifungal drug resistance." PLoS Genet **5**(10): e1000705.

Sheltzer, J. M., H. M. Blank, S. J. Pfau, Y. Tange, B. M. George, T. J. Humpton, I. L. Brito, Y. Hiraoka, O. Niwa and A. Amon (2011). "Aneuploidy drives genomic instability in yeast." Science **333**(6045): 1026-1030.

Sheltzer, J. M., E. M. Torres, M. J. Dunham and A. Amon (2012). "Transcriptional consequences of aneuploidy." Proc Natl Acad Sci U S A **109**(31): 12644-12649.

Silva, S., M. Negri, M. Henriques, R. Oliveira, D. W. Williams and J. Azeredo (2012). "Candida glabrata, Candida parapsilosis and Candida tropicalis: biology, epidemiology, pathogenicity and antifungal resistance." FEMS Microbiol Rev **36**(2): 288-305.

Singer, M. S., A. Kahana, A. J. Wolf, L. L. Meisinger, S. E. Peterson, C. Goggin, M. Mahowald and D. E. Gottschling (1998). "Identification of high-copy disruptors of telomeric silencing in Saccharomyces cerevisiae." Genetics **150**(2): 613-632.

Sionov, E., Y. C. Chang, H. M. Garraffo and K. J. Kwon-Chung (2009). "Heteroresistance to fluconazole in Cryptococcus neoformans is intrinsic and associated with virulence." Antimicrob Agents Chemother **53**(7): 2804-2815.

Sionov, E., H. Lee, Y. C. Chang and K. J. Kwon-Chung (2010). "Cryptococcus neoformans overcomes stress of azole drugs by formation of disomy in specific multiple chromosomes." PLoS Pathog **6**(4): e1000848.

Smith, J. S., C. B. Brachmann, L. Pillus and J. D. Boeke (1998). "Distribution of a limited Sir2 protein pool regulates the strength of yeast rDNA silencing and is modulated by Sir4p." Genetics **149**(3): 1205-1219.

Smith, J. S., E. Caputo and J. D. Boeke (1999). "A genetic screen for ribosomal DNA silencing defects identifies multiple DNA replication and chromatin-modulating factors." Mol Cell Biol **19**(4): 3184-3197.

Smith, S., J.-Y. Hwang, S. Banerjee, A. Majeed, A. Gupta and K. Myung (2004). "Mutator genes for suppression of gross chromosomal rearrangements identified by a genome-wide screening in Saccharomyces cerevisiae." Proceedings of the National Academy of Sciences of the United States of America **101**(24): 9039-9044.

St Charles, J., M. L. Hamilton and T. D. Petes (2010). "Meiotic chromosome segregation in triploid strains of Saccharomyces cerevisiae." Genetics **186**(2): 537-550.

Stirling, P. C., M. S. Bloom, T. Solanki-Patil, S. Smith, P. Sipahimalani, Z. Li, M. Kofoed, S. Ben-Aroya, K. Myung and P. Hieter (2011). "The Complete Spectrum of Yeast Chromosome Instability Genes Identifies Candidate CIN Cancer Genes and Functional Roles for ASTRA Complex Components." PLoS Genet **7**(4): e1002057.

Storchova, Z., A. Breneman, J. Cande, J. Dunn, K. Burbank, E. O'Toole and D. Pellman (2006). "Genome-wide genetic analysis of polyploidy in yeast." Nature **443**(7111): 541-547.

Taddei, A., G. Van Houwe, S. Nagai, I. Erb, E. van Nimwegen and S. M. Gasser (2009). "The functional importance of telomere clustering: global changes in gene expression result from SIR factor dispersion." Genome Res **19**(4): 611-625.

Takahashi, Y. H., J. M. Schulze, J. Jackson, T. Hentrich, C. Seidel, S. L. Jaspersen, M. S. Kobor and A. Shilatifard (2011). "Dot1 and histone H3K79 methylation in natural telomeric and HM silencing." Mol Cell **42**(1): 118-126.

Talbert, P. B. and S. Henikoff (2006). "Spreading of silent chromatin: inaction at a distance." Nat Rev Genet **7**(10): 793-803.

Tan, Z., M. Hays, G. A. Cromie, E. W. Jeffery, A. C. Scott, V. Ahyong, A. Sirr, A. Skupin and A. M. Dudley (2013). "Aneuploidy underlies a multicellular phenotypic switch." Proc Natl Acad Sci U S A.

Thomas, F., D. Fisher, P. Fort, J. P. Marie, S. Daoust, B. Roche, C. Grunau, C. Cosseau, G. Mitta, S. Baghdiguian, F. Rousset, P. Lassus, E. Assenat, D. Gregoire, D. Misse, A. Lorz, F. Billy, W. Vainchenker, F. Delhommeau, S. Koscielny, R. Itzykson, R. Tang, F. Fava, A. Ballesta, T. Lepoutre, L. Krasinska, V. Dulic, P. Raynaud, P. Blache, C. Quittau-Prevostel, E. Vignal, H. Trauchessec, B. Perthame, J. Clairambault, V. Volpert, E. Solary, U. Hibner and M. E. Hochberg (2013). "Applying ecological and evolutionary theory to cancer: a long and winding road." Evol Appl **6**(1): 1-10.

Thompson, S. L. and D. A. Compton (2010). "Proliferation of aneuploid human cells is limited by a p53-dependent mechanism." J Cell Biol **188**(3): 369-381.

Thorburn, R. R., C. Gonzalez, G. A. Brar, S. Christen, T. M. Carlile, N. T. Ingolia, U. Sauer, J. S. Weissman and A. Amon (2013). "Aneuploid yeast strains exhibit defects in cell growth and passage through START." Mol Biol Cell **24**(9): 1274-1289.

Thurtle, D. M. and J. Rine (2014). "The molecular topography of silenced chromatin in Saccharomyces cerevisiae." Genes Dev **28**(3): 245-258.

Timp, W. and A. P. Feinberg (2013). "Cancer as a dysregulated epigenome allowing cellular growth advantage at the expense of the host." Nat Rev Cancer **13**(7): 497-510.

Tolliday, N., M. Pitcher and R. Li (2003). "Direct evidence for a critical role of myosin II in budding yeast cytokinesis and the evolvability of new cytokinetic mechanisms in the absence of myosin II." Mol Biol Cell **14**(2): 798-809.

Torres, E. M., N. Dephoure, A. Panneerselvam, C. M. Tucker, C. A. Whittaker, S. P. Gygi, M. J. Dunham and A. Amon (2010). "Identification of aneuploidy-tolerating mutations." Cell **143**(1): 71-83.

Torres, E. M., T. Sokolsky, C. M. Tucker, L. Y. Chan, M. Boselli, M. J. Dunham and A. Amon (2007). "Effects of aneuploidy on cellular physiology and cell division in haploid yeast." Science **317**(5840): 916-924.

Upender, M. B., J. K. Habermann, L. M. McShane, E. L. Korn, J. C. Barrett, M. J. Difilippantonio and T. Ried (2004). "Chromosome transfer induced aneuploidy results in

complex dysregulation of the cellular transcriptome in immortalized and cancer cells." Cancer Res **64**(19): 6941-6949.

Waghmare, S. K. and C. V. Bruschi (2005). "Differential chromosome control of ploidy in the yeast Saccharomyces cerevisiae." Yeast **22**(8): 625-639.

Wilkening, S., M. M. Tekkedil, G. Lin, E. S. Fritsch, W. Wei, J. Gagneur, D. W. Lazinski, A. Camilli and L. M. Steinmetz (2013). "Genotyping 1000 yeast strains by next-generation sequencing." BMC Genomics **14**: 90.

Williams, B. R., V. R. Prabhu, K. E. Hunter, C. M. Glazier, C. A. Whittaker, D. E. Housman and A. Amon (2008). "Aneuploidy affects proliferation and spontaneous immortalization in mammalian cells." Science **322**(5902): 703-709.

Xu, E. Y., K. A. Zawadzki and J. R. Broach (2006). "Single-cell observations reveal intermediate transcriptional silencing states." Mol Cell **23**(2): 219-229.

Yona, A. H., Y. S. Manor, R. H. Herbst, G. H. Romano, A. Mitchell, M. Kupiec, Y. Pilpel and O. Dahan (2012). "Chromosomal duplication is a transient evolutionary solution to stress." Proc Natl Acad Sci U S A **109**(51): 21010-21015.

Yuen, K. W. Y., C. D. Warren, O. Chen, T. Kwok, P. Hieter and F. A. Spencer (2007). "Systematic genome instability screens in yeast and their potential relevance to cancer." Proceedings of the National Academy of Sciences **104**(10): 3925-3930.

Zhu, J., N. Pavelka, W. D. Bradford, G. Rancati and R. Li (2012). "Karyotypic determinants of chromosome instability in aneuploid budding yeast." PLoS Genet **8**(5): e1002719.

Zong, C., S. Lu, A. R. Chapman and X. S. Xie (2012). "Genome-wide detection of single-nucleotide and copy-number variations of a single human cell." Science **338**(6114): 1622-1626.

Appendix I

Methods for chapter 3

Yeast strains and plasmids: The yeast strains used in this study were generated in the S288c background and are listed in Table 1 and Table 4. To construct the parental strain RLY9017 (*hml::P_{URA3}-NLS-YFP*), the RLY2626 strain (*MATa, HML,* S288c background) was crossed with the Y3401 strain (*MATα, hml::P_{URA3}-NLS-YFP,* W303 background) generously provided by James Broach (Xu, Zawadzki et al. 2006). The resulting diploid strain was sporulated to obtain a haploid strain with the genotype *MATα, hml::P_{URA3}-NLS-YFP*, which was further backcrossed with RLY2626 five times to get a strain background congenic to S288c. The resulting haploid strain RLY9017 was then converted to a fully isogenic triploid strain carrying *HML::YFP* by cycles of mating-type switching and mating as described in Figure 1 - figure supplement 1A.

To obtain segregant strains from aneuploid cells, the parental strains were grown in synthetic complete (SC) medium (Sunrise Science Products, Inc., San Diego, CA) containing 25 μg/ml radicicol (Sigma-Aldrich, Saint Louis, MO) for 12 hours at 30°C and then plated on YPD plates at a single-colony density (Chen, Bradford et al. 2012). Single colonies were then selected for further analysis based on karyotype. The RLY9029 and RLY9031 strains were constructed by transforming the *Chr X::P_{gal1}-URA^{KL}-CenX* cassette, amplified from the DY6304 strain generously provided by Rodney Rothstein using primers WMP5 and WMP6, into the RLY9017 and RLY9024 strains, respectively (Reid, Sunjevaric et al. 2008). The RLY9028 and RLY9030 strains were constructed by transforming the *P_{gal1}-URA^{KL}* cassette, amplified from the RLB914 strain using primers WMP3 and WMP4, into the RLY9017 and RLY9024 strains. The RLY9033 and RLY9035 strains were obtained by crossing RLY2627 cells (*MATα, HML*) with RLY9025 cells (*MATa, hml::P_{URA3}-NLS-YFP; + Chr X*). The resulting trisomy X strain (diploid strain with

an extra copy of Chr X) was sporulated and meiotic progenies were selected for genotype *(HML-WT copy)* and karyotype, determined by qPCR, to obtain WT haploid and disome X strains.

The *LacO* array and LacI-GFP fusion protein have been described previously (Robinett, Straight et al. 1996, Straight, Belmont et al. 1996). Briefly, the RLY9041 and RLY9042 strains carrying insertions of LacI-GFP and *LacO* array 1.5 kb proximal to the *HML* locus were obtained by crossing RLY9035 (*MATa; +Chr X*) cells with the YDB111 (*MATα*) strain generously provided by James Haber (Bressan, Vazquez et al. 2004). The resulting trisomy X strain was sporulated, and the dissected meiotic progenies were selected for genotype *(hmlprox::lacO(256)-LEU2; HIS3::*P_{URA3}*-LacI::GFP-KanMX)* by growing on SC-Leu+G418 plates. WT haploid and disome X strains were identified by qPCR-based karyotyping. PCR-mediated homologous recombination was used to C-terminally tag *SIR2* with HA and mTurquoise2, tag *NUP60* with mCherry, and delete *SIR1* by replacing the genomic locus with a *KanMX6* cassette (Longtine, McKenzie et al. 1998, Sheff and Thorn 2004); correct integrations were confirmed by PCR-based genotyping.

To construct the plasmid *pWM1 (RLB912),* ORFs for *RPL39 and RPS14B* were amplified from RLY9017 cells and cloned into *EagI* and *XhoI* sites respectively, into the *pRS306* plasmid. To construct the plasmid *pWM2 (RLB913),* Gibson assembly was used to clone the indicated ORFs into the *XhoI* site of the *pRS306* plasmid. The RLY9046 and RLY9047 strains were constructed by transforming *NcoI*-digested *pWM1* and *HpaI*-digested *pWM2* into RLY9017 and RLY9018 cells, respectively. To construct the RLY9048 strain, the RLY9046 and RLY9047 strains were crossed and sporulated; the dissected meiotic

progenies were selected for the indicated genotypes using a standard PCR-based method. The plasmids used in this study are listed in Table 5.

Microscopy: To prepare cells for microscopy, yeast strains were grown in SC or drop-out medium for about 18 hours at 25°C before the cultures were diluted to a starting OD_{600} of 0.2 and grown for another five hours to an OD_{600} of 0.6-0.8. Fluorescence microscopy was performed at room temperature on live cells using a 100× αPlan Fluor NA 1.46 objective on a Zeiss Axiovert 200 M microscope (Zeiss, Jena, Germany), equipped with a Yokogawa CSU-X1 spinning-disk confocal system. Using 488 or 561 nm illumination to excite green or red fluorescent proteins, respectively, a series of optical sections with a step size of 0.5 µm was acquired with a Hamamatsu C9100 EMCCD camera and MetaMorph acquisition software. ImageJ software (v. 1.50e; NIH; RRID:SCR_003070) was used to subtract background, adjust contrast, and generate the final sum projections shown.

Time-lapse imaging was performed on a Perkin Elmer Ultraview VoX system (PerkinElmer, Inc., Waltham, MA) or a Zeiss LSM780 laser scanning confocal microscope (Zeiss, Jena, Germany) with a 63×/1.4 oil Plan-Apochromat objective and Zeiss Definite Focus. To prepare the cells, 10 µl of a mid-log phase culture with an OD_{600} of 0.5 was placed on a thin SC agarose gel pad as described (Tran, Paoletti et al. 2004). Z-stack images were acquired with a 0.5 µm step size at 30 min time intervals for 14-18 hours. For each time point, images were adjusted using ImageJ software (v. 1.50e; NIH; RRID:SCR_003070), converted to maximum Z projections, and analyzed for mean fluorescence intensities using Imaris software (Bitplane USA, Concord, MA; RRID:SCR_007370).

Induction of chromosome non-disjunction using galactose: Strains were grown overnight in SC + 2% dextrose medium, diluted 2000 times with SC + 2% raffinose medium (Sunrise Science Products, Inc., San Diego, CA), and grown to saturation at 25°C. Cells were pelleted, washed twice with water, inoculated into SC + 2% raffinose medium, and grown until cultures reached log phase with OD_{600} of 0.6-0.8. Cells were pelleted again, washed twice with water, and grown in SC + 2% galactose medium (Sunrise Science Products, Inc. San Diego, CA) for nine hours (Anders, Kudrna et al. 2009). To stop galactose induction, the cells were pelleted, transferred into SC + 2% dextrose medium (Sunrise Science Products, Inc., San Diego, CA), grown for three hours at 25°C, and imaged.

Selection of stable aneuploid karyotypes: Strains with stable aneuploid karyotypes were selected as previously described (Pavelka, Rancati et al. 2010). Briefly, DNA content was analyzed by fluorescence-activated cell sorting (FACS) for eight randomly picked colonies derived from each of the desired triploid meiosis-generated spores; strains were only selected for further analysis if the DNA content of the eight colonies showed levels of variability similar to those of the wild-type control strain RLY9017, indicating uniform ploidy. For these strains, DNA content was reassessed as before, using cells that were independently revived from frozen stocks three times. Strains that continued to show stable ploidy after repeated rounds of FACS analysis were then karyotyped by qPCR.

Illumina whole-genome sequencing: Euploid (RLY9017, RLY9019, and RLY9021) and aneuploid (RLY9071, RLY9076, RLY9078, and RLY9079) strains were subjected to

whole-genome sequencing. Genomic DNA (gDNA) was extracted from 15 ml of stationary phase yeast cultures, using a standard protocol (Hoffman 2001) with the following modifications. Three consecutive phenol/chloroform/isoamylalcohol extractions, followed by a final chloroform extraction, were performed to reduce protein and phenol contamination, respectively. The gDNA samples were then treated with 50 ng/µl affinity-purified RNase A (Thermo Fisher Scientific, Waltham, MA) for 60 min at 37°C to remove contaminating RNA. Final gDNA yields were quantified with a ND-1000 spectrophotometer (NanoDrop, Thermo Scientific, Waltham, MA). Genomic libraries were prepared according to Illumina's recommendations, except that sonication was used instead of nebulization. Cluster generation and read sequencing were performed according to Illumina's recommendations. 150 bp paired-end reads were collected using the Illumina MiSeq system (Illumina, Inc., San Diego, CA) and aligned to the UCSC sacCer3 reference sequence using the BWA package; RRID:SCR_010910 (Li and Durbin 2009), set at a maximum edit distance of 2 per read and allowing for gapped alignment with a maximum of 5 gap opens and −5 gap extensions. The genome analysis toolkit (https://software.broadinstitute.org/gatk/; RRID:SCR_001876) was used to call variants between the reference genome (sacCer3) and each of the strains. Variants were annotated using SnpEff (http://snpeff.sourceforge.net; RRID:SCR_005191). We then excluded SNPs found across all sequenced strains to eliminate mutations already present in the euploid background. All potential mutations were then manually inspected in IGV (http://www.broadinstitute.org/igv; RRID:SCR_011793), and SNPs called in repetitive regions, in long poly-A or poly-T stretches, or in regions of low alignment quality were discarded. All remaining SNPs were verified by reanalyzing each strain using Sanger

sequencing. This analysis revealed that there were no mutations in coding regions that were not already present in the parental euploid strains. Reads have been deposited in the NCBI Sequence Read Archive (SRA; RRID:SCR_004891) under accession no. SRP105283.

RNA-seq analysis: Cells were grown in SC medium for 18 hours at 25°C; cultures were then diluted to a starting OD_{600} of 0.2 and grown for five to six hours to an OD_{600} of 0.6. RNA samples were prepared from ten OD_{600} units of the final yeast culture using a standard acid–phenol/chloroform extraction method (Collart and Oliviero 2001), and contaminating gDNA was removed by treating with DNase I (Sigma-Aldrich, Saint Louis, MO). PolyA-selected, 50 bp single-end RNA-seq libraries were prepared using the Illumina TruSeq stranded mRNA sample prep kit (Illumina, Inc., San Diego, CA), quantified using a Bioanalyzer (Agilent, Santa Clara, CA), and sequenced on an Illumina HiSeq 2500 platform. Reads were aligned to the sacCer3 reference genome using Bowtie software (RRID:SCR_005476) with default alignment parameters. Read counts were normalized to chromosome copy number. The resulting binary alignment/map (BAM) files were sorted and indexed using SAM tools (Li, Handsaker et al. 2009). Differential gene expression was evaluated using the edgeR library (Robinson, McCarthy et al. 2010), and adjusted *p*-values were calculated by the Benjamini-Hochberg procedure. Reads and processed data files have been deposited in NCBI Gene Expression Omnibus (GEO) under accession no. GSE98435.

Quantitative reverse transcriptase-PCR (qPCR) analysis: RNA was extracted as described above and cDNA was prepared from 2 µg of the resulting total RNA using the

Super-Script III reverse transcriptase kit (Thermo Fisher Scientific, Waltham, MA). qPCR was performed using SYBR Green real-time PCR master mix (Quanta Biosciences, Beverly, MA) and analyzed by standard procedures (Yuan, Reed et al. 2006). Gene expression profiles were normalized to chromosome copy number. The oligos used for qPCR amplification are listed in Table 6.

ChIP-seq analysis: Chromatin immunoprecipitation was performed as previously described (Aparicio, Geisberg et al. 2005). Briefly, yeast cells were grown in 500 ml of SC medium to an OD_{600} of 0.8–0.9 and were cross-linked with 1% formaldehyde (Sigma-Aldrich, Saint Louis, MO) for 20 minutes before the chromatin was extracted. The chromatin was sonicated using Bioruptor (Diagenode, Denville, NJ) at the high setting for ten cycles of 30 sec on/off to yield an average DNA fragment size of 500 bp. Chromatin extracts were diluted in immunoprecipitation (IP) buffer and centrifuged to pellet debris; the resulting supernatant, containing the chromatin solution, was aliquoted for immunoprecipitation as follows. Chromatin was first incubated overnight with antibody at 4°C, then with Dynabeads® protein G beads (Thermo Fisher Scientific, Waltham, MA). Beads were washed several times, and DNA was recovered in elution buffer (1% SDS, 0.1 M $NaHCO_3$). Crosslinking was reversed by incubating samples at 65°C overnight, followed by protease treatment, phenol/chloroform extraction, and ethanol precipitation of the recovered DNA. Sequence libraries were constructed and validated using the Illumina library protocol and sequenced using the Illumina HiSeq 2500 system as 50 bp single-end reads. Reads were mapped to the sacCer3 reference genome using Bowtie software (RRID:SCR_005476) with parameters: --best –strata -v2 -m 1. Peaks were called by

Model-based Analysis of ChIP-Seq (MACS2) using default settings (Zhang, Liu et al. 2008), mapped to the closest gene, and kept only if they occurred within 600 bases of the transcription start site. Peak scores, defined as the -log10 transformed q-values, normalized to chromosome copy number, were converted to Z-scores for comparison across strains and plotted as the difference between disome X and WT haploid strains (Figure 6A-B). Antibodies used for immunoprecipitation are: anti-HA (12CA5, Sigma-Aldrich, Saint Louis, MO; RRID:AB_514505), anti-H3K79me3 (ab2621, Abcam, Cambridge, MA; RRID:AB_303215), anti-H3K4me3 (04-745, EMD Millipore, Temecula, California; RRID:AB_1163444), and anti-H4K16ac (07-329, EMD Millipore, Temecula, California; RRID:AB_310525). Reads and processed data files have been deposited in NCBI Gene Expression Omnibus (GEO; RRID:SCR_005012) under accession no. GSE98282.

Pheromone sensitivity assay: For cell cycle analysis, 10^7 mid-log phase cells were grown in SC medium containing 2 µg/ml α-factor (US Biological, Salem, MA) for 90 mins at 30°C. Cells were then fixed in 70% ethanol and analyzed for DNA content using an Attune NxT flow cytometer (Thermo Fisher Scientific, Waltham, MA) as described (Pavelka, Rancati et al. 2010). For the halo assay, 15 µl of 2 µg/ml α-factor was applied to filter discs centered on a lawn of *MATa* cells with a WT *HML* locus. Cells were grown for 2-3 days at 30°C, and the size of the halo (region devoid of cell growth) was determined as described previously (Cherkasova, Lyons et al. 1999).

Gain-of-function screen: 304 of the 356 total Chr X ORFs are available in the Molecular Barcoded Yeast (MoBY) ORF plasmid library (Ho, Magtanong et al. 2009) and used for

the screen. Each plasmid was extracted and transformed independently into the disome III strain RLY9023 (*HML::*P_{URA3}*-YFP*) as described previously (Chen, Mulla et al. 2015). Transformants were grown in 96-well deep-well blocks containing 2 ml SC-Ura medium at 30°C for 12 hours. Cells were then fixed with 1% paraformaldehyde and imaged on the Operetta high-content imaging system (PerkinElmer, Inc., Waltham, MA) with a 63×/1.4 Plan-Apochromat objective. Desilencing scores were calculated as the ratio of the mean YFP fluorescence intensity of a test strain carrying a MoBY plasmid to that of the disome X strain carrying an empty MoBY vector (RLY9046).